UNIVERSITY OF TRENTO

International PhD Program in Biomolecular Sciences

30th Cycle

"Droplet based synthetic biology: chemotaxis and interface with biology"

Tutor

Prof. Martin M. Hanczyc

CIBIO University of Trento

Ph.D. Thesis of

Silvia Holler

CIBIO University of Trento

Academic Year 2018-2019

I, Silvia Holler, confirm that this is my own work and the use of all material from other sources has been properly and fully acknowledged.

Abstract

Life-like behaviors such as fission, fusion and movement can be artificially re-created exploiting highly simplified protocell systems. This thesis is mainly focused on chemotaxis protocell systems and their integration with biological systems in order to show potential future applications. 1-Decanol droplets, formed in an aqueous medium containing decanoate at high pH, become chemotactic when a chemical gradient is placed in the external aqueous environment. We investigated the behavior of these droplets, their ability to transport and deposit living and non-living objects and to interface them with biofilms. To make the artificial system compatible with natural living systems we developed a partially hydrophobic alginate capsule as a protective unit that can be precisely embedded in a droplet, transported along chemical gradients and deposited. We developed a system that was able to transport: *Escherichia coli*, *Bacillus subtilis* and *Saccharomyces cerevisiae*. Both bacteria survived the transport. However, yeast survived but not in a consistent and repeatable way. Next, we evolved the system to transport human cell lines. We found that A549 cells survive encapsulation but not the transport. A549 cells are in fact very sensitive to toxic 1-decanol. We however found out that this cell line secretes compounds able to decrease the surface tension and to increase the capsule-droplet affinity. Finally we discuss future solutions for the effective transport of human cells.

Contents

Chapter 1

Introduction

Artificial life is recently gaining more and more interest in the scientific world [1]. The bridge between life and non life is very thin. Life-like behaviors such as fission, fusion and movement can be artificially re-created exploiting highly simplified protocell systems. This systems are examples of bottom-up synthetic biology. Bottom-up synthetic biology was defined by Leduc in 1914 as an approach where properties of living matter are recreated from "the simpler to the more complex, beginning with the reproduction of the more elementary vital phenomena" [2].

The term protocell has been used loosely to refer to the first cells or to primitive cells. Here we will use this term to refer to aggregates such as vesicles and droplets in water showing life like behaviours. Droplet are compartments that create mixing two immiscible fluids, oil has for example the characteristic to auto-assembly in water due to its hydrophobic nature. However, one of the most popular ways of making a protocell are vesicles, supramolecular amphiphilic aggregates with a water interior. Vesicular protocells can be quite simplistic yet serve as semi-permeable barriers and define different types of compartments in a water based environment. Vesicles can show life like behaviours such as growth and division [3]. This is for example the case in which one equivalent of myristoleate micelles is added to myristoleic acid/ myristoleate vesicles [3]. Extremely reducing the cell to a membrane containing RNA and the reproduction to the generation of two vesicles from one, a single vesicles can exhibit a reductionist reproduction over multiple generations. Tsuji et al. 2016 [4] demonstrated the sustainable proliferation of liposomes that replicate RNA within them. Nutrients for RNA replication and membranes for vesicle growth were combined and showed fusion and fission behaviour compatible with RNA replication and distribution to daughter protocells. It is however missing in this type of protocell the 'building blocks' production. Nutrients for RNA synthesis and vesicle formation are in fact previously synthetized. We can also consider that when RNA is encapsulated inside compartments, it can exert an osmotic pressure on the vesicle membrane which drives the membrane growth through an increase in the uptake of membrane components. RNA replication could cause faster cell growth inside protocell and this could be considered as a starting principle for cell evolution [5]. Protocell-like compartments can even be created using another type of amphiphilic compound: proteins. Li et al. [6] showed that protein-polymer building blocks can auto-assemble and exhibit cell-like properties such as molecule encapsulation, catalysis by internalized enzymes and selective permeability.

Another leading property of cells and living organisms is the ability to move. Protocell like moving systems can be created by simple chemical mixes: using for example droplet of oil in water or water

in oil. Droplets of oil in water were first described by Otto Bütschli in 1898. He used alkaline water droplets in olive oil to initiate a saponification reaction. This simple protocell system recreated an entity that moved and seemed to behave like an amoeba. Since then many researchers have been developing oil droplet systems as models of living systems. For example, the research of the group of Hagan Bayley in Oxford created 3D customized patterns of water droplets in oil with stable lipid bilayers forming the droplet-droplet interfaces as mimics of living tissues. In addition these networks of droplets with integrated porins can show current transmission. Each droplet in this system can be complemented even with cell-free expression systems controlled by light activating protein expression [7]. In this way they demonstrated that life-like behaviours such as current transmission and protein expression can be activated even in water-in-oil droplets. Such droplets and their bilayer interfaces could be considered as a minimalist reduction of living tissues However it is not clear the relationship between this droplet system and origin of life context.

During my PhD, I mainly focused my attention on protocell chemotactic system of oil droplets in water. The water phases 'environments' in which these droplets are manually placed contain surfactants. Surfactants are biological compounds with amphiphilic nature and can be divided in three categories: anionic, cationic and non ionic. Starting from knowledge transfer I reproduced chemotactic systems of 1-decanol droplets moving in salt gradients [8, 9] and on this protocell system I mainly focused my activity. I would like to underline that the focus of this thesis is not to gain information about the origins of life and protocell generation, but instead the creation of an artificial life system, showing the life-like behaviour of chemotaxis, starting from simple chemicals in the laboratory. This artificial life system will be interfaced with living organisms (going from bacteria to eukaryotic cells) and can be used perhaps one day for the development of new technologies.

1.1 Types of cell motility

The normal length of living cells goes from 7-8 to 120 micrometers for the cell body. Only in the case of neurons, considering even the axon, we can reach dimensions of 1m (in the case of humans). The little dimensions of cell bodies are compatible only with high Reynolds numbers, so the motion of a cell requires the use of energy. However some cells still rely upon passive flotation and Brownian motion for their dispersion. In some specific conditions, for example, cells move randomly due to the molecular bombardment by the solvent molecules. This type of undirected motion demands no energy nor sophisticated machinery from the cells and is called random motility. Furthermore, there are several primary mechanisms of active cell motion: swimming using rotating flagella in prokaryotes, e.g. *E. coli*, or cilia in eukaryotes, *Tetrahymena*; cytoskeleton polarization, e.g. *Dictyostelium*; and gliding, cyanobacteria.

The cell motility can be divided into three types [10]: basal random motility (which takes place in the absence of chemical stimuli), chemokinesis (which corresponds to increased random motility in response to chemical stimuli) and chemotaxis, which corresponds to stimulated migration towards an increasing (or decreasing) chemical gradient. Chemotaxis was first described more than a century ago, by T.W. Engelmann in 1881. He observed the movement of bacteria towards the chloroplasts in a strand of Spirogyra and hypothesized bacteria were moving in response to the oxygen released from chloroplasts. Afterwards, Pfeffer W. [11] observed, in 1884, chemotactic accumulation of bacteria in response to gradients created by glass capillaries.

1.2 Sensing in biology

Organisms to survive do not simply move in response to chemicals but even for example in response to thermal and oxygen gradients. Specifically, most organisms (even bacteria) can sense light, pressure, temperature and chemicals and as a response display specific movements (phototaxis-response to light [12], magnetotaxis-response to magnetic field [13], thermotaxis-movement along thermal gradient [14], galvanotaxis-movement along the electric field [15], haptotaxis-movement along the gradient of adhesion sites [16], gravitaxis-movement along the direction of the gravitational force [17]). Intelligent animals can find food by coordinating their senses with their central nervous system. Small organisms with no sense-specific organs or central nervous system find food by chemotaxis. The bacterium *E. coli* can sense and respond to changes in temperature, osmolarity, pH, noxious chemicals, DNA-damaging agents, mineral abundance, energy sources, electron acceptors, metabolites, chemical signals from other bacteria, and parasites [18]. There are two modes of chemical gradient sensing: temporal and spatial. Bacteria are very small organisms and, due to their length scale, are not able to detect gradients spatially, therefore they detect the chemicals temporally [19, 20]. Eukaryotic cells are instead bigger than bacteria, and can sense, through their receptors in different positions on cellular membranes, chemical gradients spatially. A well described system of eukaryotic chemotactic is for example the migration of *Dictyostelium amoebae* along an increasing concentration of cyclic adenosine-3′,5′-monophosphate (cAMP) [21]. A *Dictyostelium* cell can measure about 1% of concentration difference of cAMP over its total length (10-20 μm). *Dictyostelium* cells perform a random type of motion with the average motility 4.19 μm/min [22] in the absence of cAMP and show no directional response to negligible stationary, linear cAMP concentration gradients (of less than 10^{-3} nM/μm). In steeper gradients, cells can reach an average velocity of $\sim$9 μm/min towards the cAMP source.

1.3 Importance of chemotaxis in multicellular organisms

In multicellular organisms, chemotaxis is very important in physiological processes, such as the recruitment of inflammatory cells to sites of infection and in organ development during embryogenesis [23]. Neuronal and embryonic cells migrate during development. During angiogenesis, endothelial cells undergo chemotaxis to form blood vessels, while epithelial cells and fibroblasts chemotaxis during wound healing [24]. In addition, chemotaxis governs the motion of sperm towards the egg during mammalian fertilization. For healthy neurons and epithelial cells, micromolar concentrations of gamma-aminobutyric acid (GABA) induce chemokinesis in rat cortical neurons during development, while femtomolar concentrations induce chemotaxis [25]. Furthermore, vascular endothelial growth factor A (VEGFA) was shown, using microfluidic chemotactic chambers, to increase chemotaxis of epithelial cells while decreasing chemokinesis [26]. However, in addition to a role in obviously beneficial processes in multicellular organisms, chemotaxis is also involved in each crucial step of tumor cell dissemination and metastatic progression (invasion, intravasation and extravasation). Many cancer cells such as breast cancer cells are known to preferentially metastasize into certain tissues and organs. This preference is correlated with the production of chemoattractants by the target tissues and organs and up-regulation of chemoattractant receptors in the cancer cells [27].

1.4 Moving soft matter systems

The development of soft matter systems that mimic the behavior of living systems [28] can be useful in studying related processes in natural living systems and also in pioneering new materials [29] and technological designs [30]. Soft matter systems can be driven out of equilibrium and can show large responses to external stimuli [31]. The switch from equilibrium to non equilibrium systems can be driven through, for example, static external fields, externally imposed physical shear flows, or chemical potential. There are many soft matter systems that show the ability to move. Some self propelled oil droplets showed for example the ability to move randomly: 4-octylaniline oil droplets containing 5 % moles of an amphiphilic catalyst exhibited a self-propelled motion inside an aqueous dispersion of 4-octylaniline [32].

Some self-moving systems also shown the ability to move directionally in response to chemical signals in the environment and therefore such systems are capable of chemotaxis [33]. Droplets of 0.5 M oleic anhydride in nitrobenzene when placed in oleic anhydride solution start hydrolyzing, waste product is created, convective flow generates inside the droplet and droplet moves directionally in response to it, to its waste product creation and to pH decrease. The movement of the droplet, away from its waste product and towards fresh unmodified oleic acid solution could be considered as a primitive form of chemotaxis. The environment in which the droplet move can even be modified and become complex. 2-hexyldecanoic acid (HDA) in dichloromethane (DCM) (20 % w/v) droplets show for example an efficient chemotaxis when placed inside a maze in which an acid source is placed and a pH gradient is created [34].

1.5 Chemotaxis systems

Chemotaxis, defined as a stimulated migration towards an increasing (or decreasing) chemical gradient, can be re-created artificially using protocell systems. There are many systems in which chemotaxis is created in response to a pH gradient. When an oleate anhydride droplet is placed inside an high pH (12) oleic acid environment, it undergoes hydrolysis and the waste product creates a pH decrease that induces the droplet to move [36, 37]. Therefore droplets in this system move in response to the self-generated pH gradient. This kind of behaviour is reported in Figure 1.1 (the figure is obtained from M.M. Hanczyc, Prebiotic metabolism and motility (2010) [37]).

Droplets in this system move in response to its self-generated pH gradient. As shown by Hanczyc et al. [33, 37] oleate anhydride droplets move even in response to an external pH gradient. Other types of droplets can instead move, not only away from, but even towards region of lowered pH: 2-hexyldecanoic acid (HDA) in dichloromethane (DCM) (20 % w/v) droplets, when placed inside a maze [34], move towards the point of acid source. Chemotaxis can happen even in response to sources of chemical compounds. Cejkova et al. showed in 2014 1-decanol chemotaxis towards a salt source. They covered the edges of a microscopic slide with thin strips of adhesive to create upon a glass slide a pool filled with 1 mL of decanoate (5 or 10 mM). Afterwards they placed a 5 μL decanol droplet, added 10 μl 5 M NaCl (on the opposite side respect to the droplet) and created a chemical gradient towards which the droplet migrated [9]. This systems works even in mazes [9] and can be exploited to transport non living [35] and living [38] objects. Jin et al. showed in 2017 that an oil phase consisting of the nematic liquid crystal of 4-pentyl-4'-cyano-biphenyl move towards tetradecyltrimethylammonium bromide (TTAB) source [39]. The chemicals that induce the chemotaxis can even appear in gas phase: oleic acid droplets showed negative chemotaxis in response to nitrogen gas [40]. As demonstrated by all these works protocell like

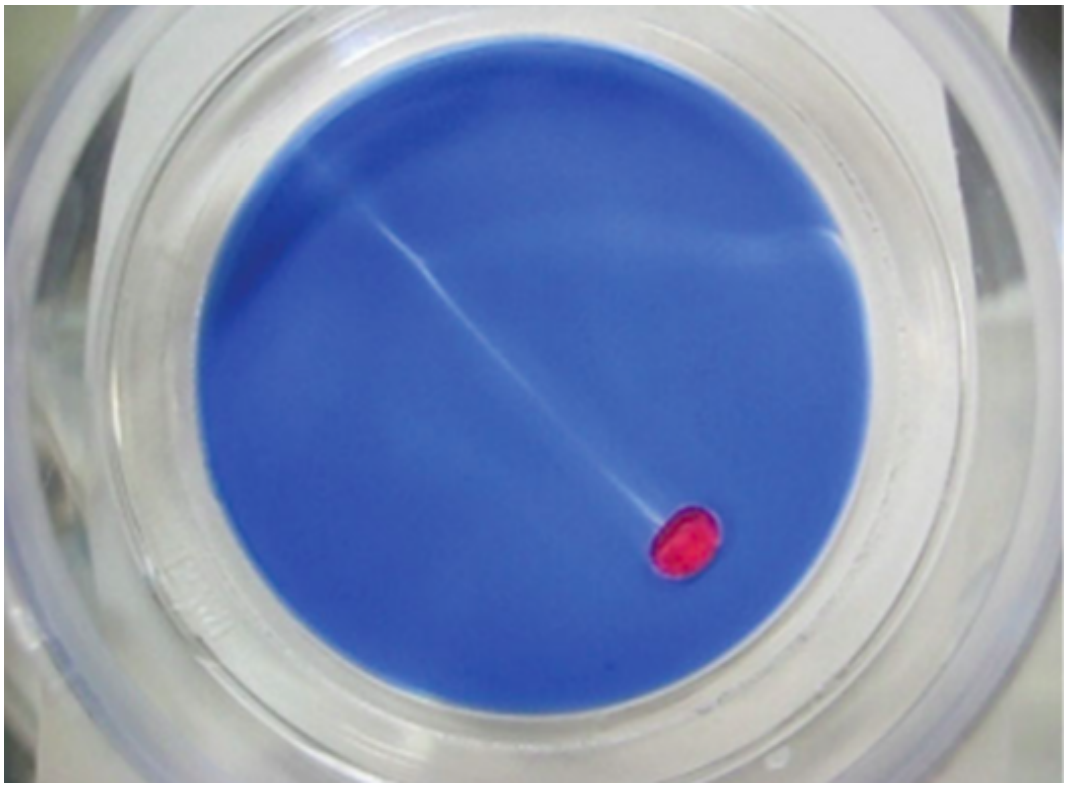

Figure 1.1: **Oleic anhydride self propelled chemotaxis.** Nitrobenzene (NB) droplet containing 0.5 M oleic anhydride (colored using Oil Red O) placed in a glass-bottom disc containing 10 mM oleic acid pH 12 to which was added a pH indicator, thymolphthalein. The pH indicator is blue at high pH and colourless below pH 11. As soon as the droplet is placed in the water phase, oleic anhydride starts hydrolyzing and creates a waste product that decreases the pH, the droplet moves away from its starting position and a white trail is left behind the droplet [37].

structures can show chemotactic behaviour. This can happen in response to: pH, chemicals (simple as NaCl or complex as TTAB) and gases.

This thesis describes a model of synthetic biology based on liquid droplets. Chapter 2 describes chemotaxis, its general explanation, the experimental settings, chemotaxis in a 3D environment, the transport of small objects and multi-droplets 'multi' objects transport. Chapter 3 and 4 present the integration of chemotactic droplets with living systems. In chapter 3 droplets are used for the transport and deposit of capsules containing *E. coli, B. subtilis and S. cerevisiae*. In chapter 4 droplets are used for the auto-selective transport of living eukaryotic cells (i.e. A549 cells). Chapter 5 describes the integration of chemotactic droplets with living biofilm, microbial fuel cells and magnetic nanoparticles. Chapter 6 characterizes the droplet movement, describes automated droplet tracking and evolutionary algorithms applied to the droplet system. To conclude in Chapter 7 future perspectives are presented.

Chapter 2

Chemotaxis

This next section is based on the droplet chemotaxis work by Cejkova et al. 2014. Droplet motion will be described and characterized in a 2D and 3D environment and as well as a vehicle for the transport of light objects.

2.1 Experimental settings of decanol droplets chemotaxis experiments

The taxis system we used is composed of a 1-decanol droplet and a surrounding environment of decanoate solution (typically 5 mM, pH 11-12). A chemical gradient is then created with the addition of sodium chloride (usually 3 M NaCl) and the droplet moves chemotactically towards the gradient source. The explanation of this motile droplet system has been published in [9] describing how changes in interfacial tension govern the motion and direction on the droplets. The droplet moves from a starting position to an end up one in which its interfacial tension, with the surrounding environment, is reduced. There are even other forces taking part in this complex systems such for example: interactions between the sodium salt ions and the surface of the 1-decanol (supposed to be negatively charged due to the high pH of decanoate solutions), the marangoni flow created in inside the droplets by this interaction and the convective flows created in decanoate from the movement of the droplet itself. The design of the test system is depicted in Figure 2.1: A droplet of 1-decanol is placed at the starting point A, and then the salt is deposited in target position B. This shows that the directional motion of the droplet is dependent on the salt gradient, as previously described [9] and is consistent with the system finding the lowest energy state (Figure 2.2).

2.2 Results

2.2.1 Surface tension

The data obtained for the surface tension liquid phase analysis are following reported. Decanoate was mixed with NaCl solutions (at different molarities) and effect of increasing NaCl concentration and the subsequent interfacial tension reduction is shown in Figure 2.2.

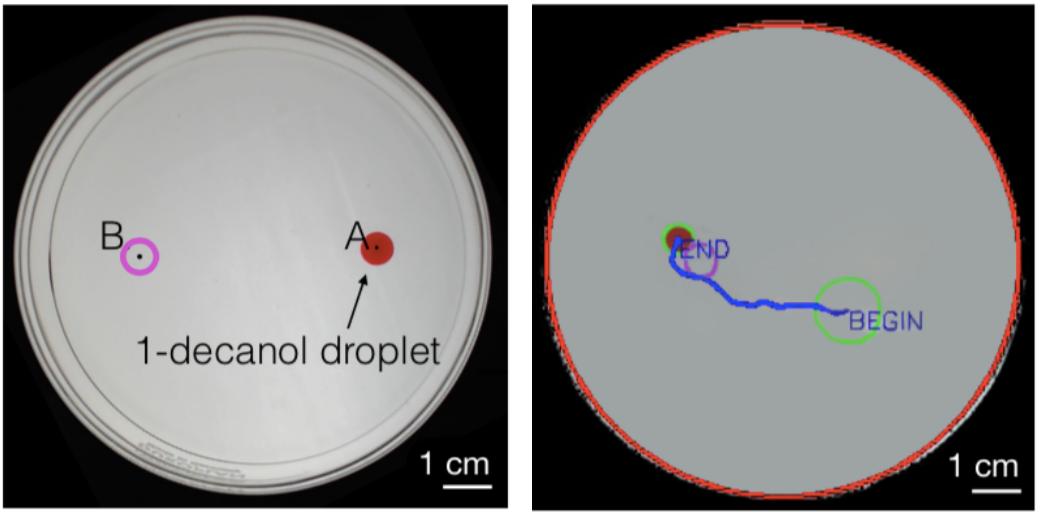

Figure 2.1: **General design of droplet-mediated transport experiment and tracking.** (a) The diameter of the glass Petri dish is 90 mm. 9 ml of 5 mM decanoate pH 11 solution was added to the dish. The 1-decanol droplet, colored with Oil Red O for easy visualization, was added at position A. Salt is added at position B to create the gradient. (b) The migration of the droplet is monitored with a video camera and the lateral movement is recorded, see Methods. The droplet path is shown as a blue line generated by the tracking algorithm. See chapter 6

2.2.2 3D chemotaxis

So far most chemotactic droplet studies demonstrate movement in 2D. The 1-decanol droplet system was modified to work even in a 3D environment. A sucrose gradient was created inside a beaker using decanoate solution alone or mixed with sucrose 2 M and colored with bromophenol blue, this in way to obtain two separated phases of different density (bromophenol blue was added only to the sucrose enriched decanoate to check by eye for the density gradient). A droplet of the chloroform-1-decanol (1:1 mix) was added to the beaker and placed itself in the middle of the two phases due to their density differences. Without sucrose gradient 1-decanol-chloroform droplet would have laid on the bottom of the water phase interacting with the glass of the petri dish, because its density is roughly 1,16 g/cm^3. We chose to use this decanol-chloroform mix to vary as little as possible the droplet composition while changing its density (1-decanol was maintained and its density was increased using chloroform). We did not test instead halogenated variants of decanol (that have a higher density compared to 1-decanol) because of their exceptionally high cost. Starting from this settings, when 3 M NaCl was added inside the beaker (on the opposite side were the droplets were placed) droplets showed a migration towards the salt source. An example of the experimental setting and a droplet that moves towards the salt source is shown in Figure 2.3.

We previously tested even the 3D chemotaxis of decanol-chloroform droplets with density of 1 g/ml in pure decanoate solution. When this kind of droplets are placed in decanoate, they start losing their chloroform counterpart, due to the fact that chloroform is slightly soluble in water, and move to the air water interface. This is the reason why we preferred to use a wider density gradient (almost 1 g/mol for decanoate and 1,253 for 2 M sucrose) in which our decanol-chloroform 1:1 mix would have been retained stably in its middle for a longer time.

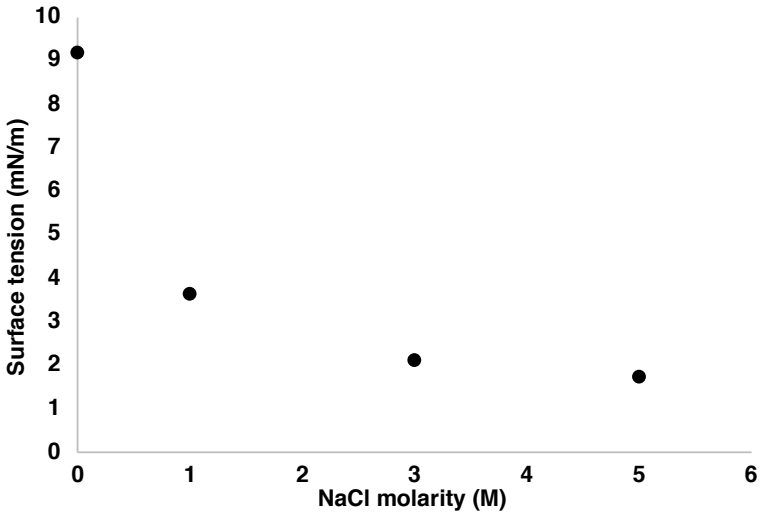

Figure 2.2: **Surface tension of 1-decanol in different aqueous phases.** Surface tension (in mN/m) for 1-decanol inverted pendant drop in: decanoate 5 mM pH 11.5 and decanoate 5 mM pH 11.5 mixed 1:1 with NaCl 1, 3, or 5 M. Error bars correspond to standard deviation of 10 replicates. Error bars not visible; standard deviation for each point ranged from 0.04 to 0.08 mN/m.

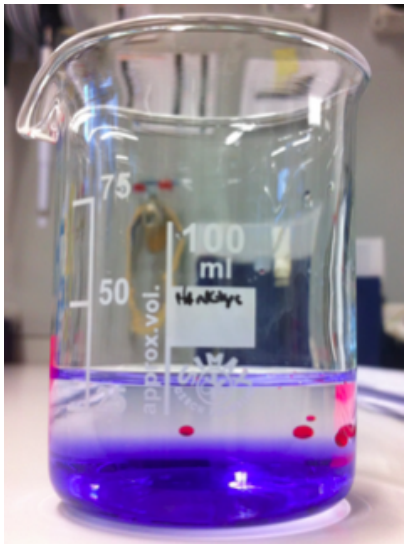

Figure 2.3: **3D chemotaxis experiment** Chloroform-1-decanol droplets migrating from right to the left side of the glass beaker inside a sucrose gradient

2.2.3 Chemotaxis and transport of small objects

It was shown by Cejkova et al. 2014 that chemotactic droplets could serve as transporters for chemicals [35]. I investigated the use of decanol droplets to transport small light objects such as pieces of copper wire, of parafilm, of plants' leaves and dried alginate capsules. Decanol droplet system was shown to efficiently move several times and deposit a small piece of copper wire, this on demand through the addition of 25 mM decanoate in water (pH 12) to the system (see Figure 2.4).

Small pieces of copper wire (mean length 1.5 mm) were cut using scissors. Decanoate solution (9 ml) and 1-decanol droplet 20 μl was placed inside a petri dish and using tweezers the copper wire was placed upon the droplet. Afterwards the salt gradient was created using 100 μl 3 M NaCl and the droplet moved

towards the salt source transporting the copper wire. Droplet-copper wire interaction was destabilized through the addition of 1 ml (in total) of 25 mM decanoate pH 12. For the second chemotactic movement 200 μl of 3 M NaCl were added. In this case for the final drop of the copper wire 600 μl of 25 mM decanoate solution were needed. The last chemotactic movement was achieved with 100 μl 3 M NaCl (all the movements are reported in Figure 2.4). Being the second droplet chemotaxis in an already salty environment more salt solution is needed for the droplet to sense the gradient. We can instead observe that for the last chemotaxis a lower amount of salt is necessary, this probably due to the fact the movement of the droplet is easier once it has released its cargo. It has been in this way showed that 1-decanol droplets can be used to transport and release non-living objects such as a piece of copper wire.

2.2.4 Multiple droplet chemotaxis and transport of multiple objects

Inside an enclosed environment such as a petri dish, multiple droplets can show chemotaxis simultaneously. One of the objects that can be transported using 1-decanol droplets are alginate capsules. Capsules are created using alginate 5 % w/v, dropped with syringe in $CaCl_2$, cross-linked and dried overnight (droplets are colored using bromophenol blue for an easier visualization). A video of multiple decanol droplets transporting multiple alginate capsules can be found at: `https://youtu.be/nJJTD7EpMws`. All the droplets move chemotactically after the addition of salt solution (3 M, blue to the addition of bromophenol blue) and can carry different number of droplets: none, one or two (see `https://youtu.be/ejtFx2nQiaI`). The same kind of transport system works even with alginate capsules transported by oleic acid droplets and moving away from a point in the petri dish in which HCl 1 M is added (see `https://youtu.be/WQOSKTVYKBk`). It was even found that by increasing the volume of the droplet the number of the capsules that can be transported increases too. For example, a droplet of 30 μl can transport 8 alginate capsules.

2.3 Discussion

We started from a previously tested chemotaxis system [9] and optimized it to obtain capsule directed movement in petri dishes. We analyzed the forces driving the chemotaxis movement and explained it with surface tension reduction induced by sodium chloride solution addition. The system was at this point evolved to transport objects. This objects had to be light and small in way that once manually place upon the 1-decanol droplets (at air water interface) they wouldn't have been instantaneously dropped. We showed in this chapter that we transported both two pieces of copper wire and alginate capsules. The chemotaxis transport is efficient and can be driven to a previously selected point. We have until now tested only 2D chemotaxis systems but showed that it can be performed in a 3D one. This system has to be developed in way to be more stable, decanol-chloroform droplets for example loose their chloroform higher density part while incubated in the sucrose gradient. For what concerns this part of work, feasible future perspectives could be the transport of other small objects and the test of other 3D systems using different oil phases with increased densities, glycerol could for example used for this purpose.

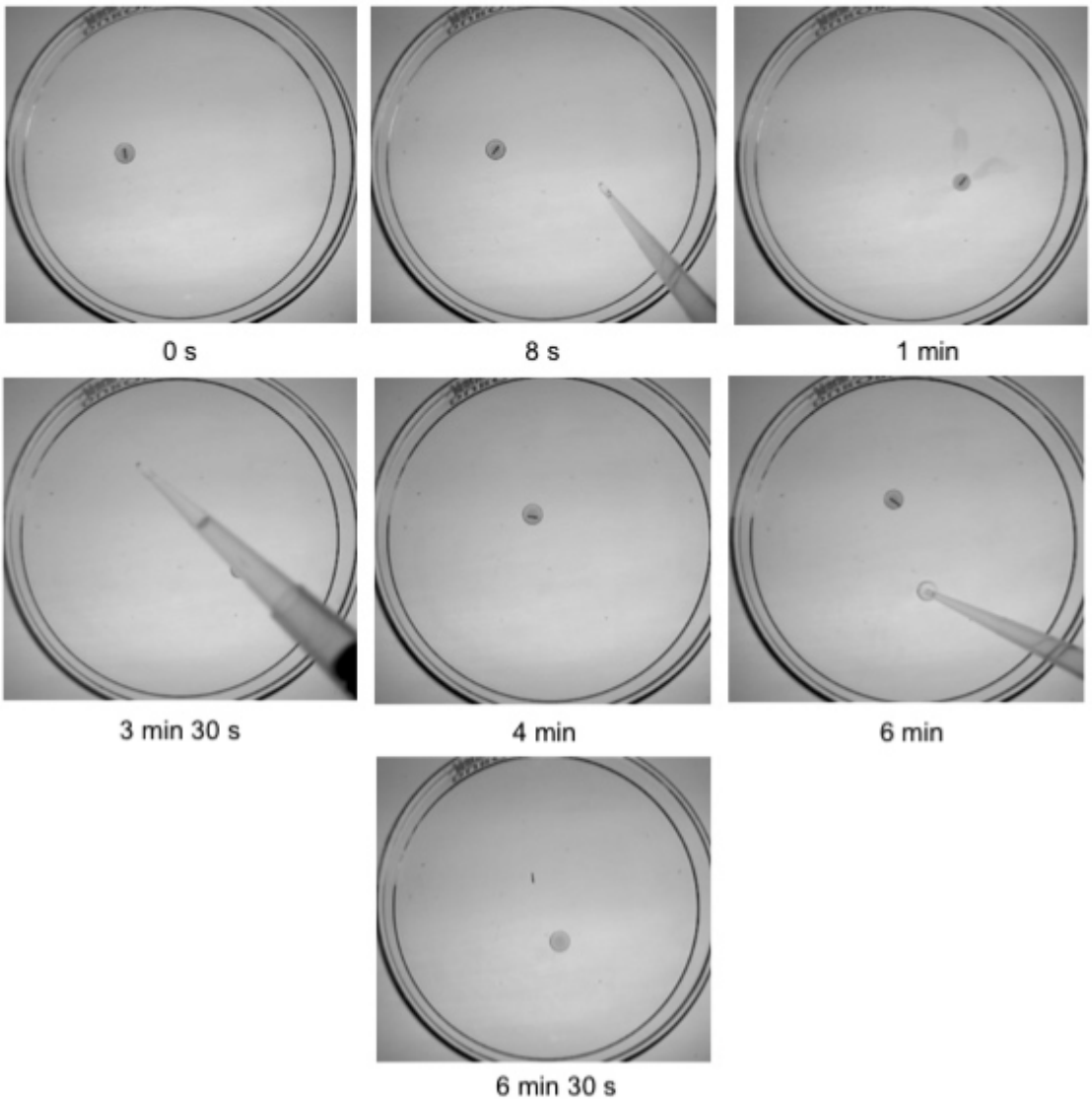

Figure 2.4: **Chemotactic transport of a piece of copper wire** Decanol droplet transporting and dropping a piece of conductive copper wire of 1.5 mm in length. The diameter of the glass petri dish is 60 mm. 0 sec: droplet with wire placed in experiment; 8 sec: salt gradient added; 15 sec – 1 min: droplet migration towards salt source; 1 min – 3 min 30 sec: 25 mM decanoate addition; 3 min 30 sec: second salt addition; 3 min 30 sec – 4 min: droplet migration towards second salt source; 4 min – 6 min 25 mM decanoate addition to trigger release of wire from droplet; 6 min third salt addition; 6 min – 6 min 30 sec migration towards third salt source and wire left behind. See movie at 8× real time [`http://youtu.be/l3aAjdjQ0m0`].

2.4 Material and Methods

Material

All reagents for the chemotaxis experiments were supplied by Sigma Aldrich: decanoic acid, 1-decanol, Oil red O, sodium hydroxide, bromophenol blue, sodium chloride, calcium chloride and sodium alginate. Glass DURAN Petri dishes were supplied by Fisher, syringes from PIC and Glass slides from Prestige.

Methods

Experiments were carried out at room temperature.

2.4.1 1-decanol chemotaxis

Glass Petri dishes of 9 cm diameter were filled with a volume of 9 ml 5 mM decanoate solution pH 11 (adjusted with 3 M sodium hydroxide (NaOH)). Droplets of (20 μl) 1-decanol (colored with Oil red O, in a random desired concentration depending on the color we wanted to obtain) were manually added to the system. The object to be transported (dehydrated alginate capsules or copper wires) were placed manually on the decanol droplets. The chemotactic movement of the droplets was obtained through 3 M sodium chloride (NaCl) addition as previously described in Cejkova et al. 2016 [9]. Wire deposition was done through the addition of a decanoate solution with a higher molarity (0.2 M pH 12) near the droplet. Droplets were then moved a second time through the addition of 3 M NaCl. In the case of 3D chemotaxis 1-decanol-chloroform 1:1 mix was created, colored with Oil red O, drops of varying volumes were added thought the use of a glass pasteur pipette and stopped at the interface between the two phases (decanoate 5 mM pH 11 and decanoate 5 mM pH 11 with the addition of 2 M sucrose and bromophenol blue). System was moved using 3 M NaCl.

2.4.2 Inverted pendant drop surface tension

1-decanol (pure) inverted pendant drop surface tension was analysed inside different water phases: decanoate 5 mM pH 11.5 and decanoate 5 mM pH 11.5 mixed 1:1 with NaCl 1, 3, or 5 M. Data were obtained for ten droplets (of 4-5 μl) for each condition using a hooked needle (gauge 22), Theta-lite tensiometer Attension by Biolin Scientific (Nordtest Srl, Italy) and a high precision cell with optical path of 10 mm by Hellmark analytics.

2.4.3 Alginate capsules preparation

Alginate was dissolved in water (5 % with the addition of bromophenol blue) capsules crosslinked in 1 % w/v calcium chloride and dried overnight.

To summarize, we characterized the 1-decanol chemotaxis in NaCl salt gradients, from a starting position A to a pre-decided location B. We analyzed 1-decanol surface tension reduction in a salt environment and explained chemotaxis through energy minimization. We then placed the 2D chemotactic droplet in a 3D sucrose gradient system. Finally decanol droplets were exploited to transport light objects such as pieces of copper wires and alginate capsules. We speculated at this point if we could use the alginate capsules to entrap and protect living cells, we could use this droplet system to directionally transport living cells, as tested in the next chapter.

Chapter 3

Integration of chemotactic droplets with living systems

Knowing the feasibility to transport small inorganic objects we had the idea to try to evolve the chemotaxis system to integrate even with the living system, starting from example from the transport of living cells.The experimental conditions that support the chemotaxis, such for example high pH, the presence of surfactants and the own toxicity of 1-decanol, may be detrimental for the sustenance and proliferation of living organisms. Knowing that simply resuspending cells in 1-decanol would have led to cell death and that placing a water based cell resuspension directly on decanol would have resulted in droplet split with the release of cells, we tried to create a protective shell to transport cells. We required a shell with the following characteristics: able to protect the cells from the surrounding environment, with the feasibility to be coupled and decoupled from 1-decanol and easy to be dissolved. There are many types of protective capsule that we could have used, such as the ones based on hydrophobic coatings [41] or on self-assembled short peptides [42]. We decided to use sodium alginate for its ease.

Sodium alginate is a polysaccharide obtained from brown seaweed and two kinds of bacteria (*Pseudomonas* and *Azotobacter* [43]. Alginate is a compound with a broad use in biomedical applications and bio-engineering [44]. Typically alginate is prepared in water and cross-linked forming a hydrogel. Alginate hydrogels are exploited for different applications: wound healing, drug delivery, *in vitro* cell culture and tissue engineering. Alginate produces safe and reliable effects in many applications, for example in the treatment of type 1 diabetes [45], treatment of urinary incontinence and vesicoureteral reflux [46], treatment of anemia [47], treatment of brain tumor [48], and cryopreservation [49]. In addition, alginate hydrogels can be applied to diverse applications when modified [50] or when integrated with other types of gels able to respond to pH or temperature stimuli [51]. We will use sodium alginate, cross linked using calcium chloride, to create a protective shell in which cells are encapsulated.

However, alginate is by composition too hydrophilic for stable integration into the hydrophobic 1-decanol droplets. Several alternatives for using chemically modified hydrophobic alginate exist and require chemical synthesis and purification or extreme chemical modification. For example cold plasma treatment could be used to create alginate surfaces with hydrophobic properties [52, 53]. In addition, several alginate derivatives have been synthesized to create an amphiphilic alginate that requires the chemical modification of the alginate backbone by alkyl chains and other hydrophobic moieties [44].

I experimented with a simple solution to physically integrate an alginate capsule containing live

cells into hydrophobic droplets by adding a surfactant (decanoate in different concentrations) during the hydrogel crosslinking step. I simply dissolved alginate at the 5% w/v in different decanolate solutions at pH 12 ranging from 5 to 25 mM. This method resulted in an alginate hydrogel with definable hydrophobicity by simply titrating the amount of surfactant added. This solution has the added benefit of being easily dissolved allowing for release of the cargo. I tested various cells for compatibility with the chemical system including *Escherichia coli (E. coli)*, *Bacillus subtilis (B. subtilis)*, *Vibrio fischeri (V. fischeri)* and *Saccharomyces cerevisiae (S. cerevisiae)*. The cells were temporarily placed in a biocompatible capsule as a protective environment but also as a measurable and well defined unit of cargo for transport. We then used the self-moving 1-decanol droplets as vehicles to transport the hydrophobic alginate capsules. A droplet with one or more alginate capsules was able to move chemotactically in salt gradients. After transport, the association between the alginate capsule and the decanol droplet was disrupted, and the alginate capsules were harvested from the system. We show that *E. coli* and *B. subtilis* cells were alive and proliferate after droplet-mediated tactic transport under otherwise sterile conditions.

3.1 Results

3.1.1 Alginate capsule design

We prepared the alginate capsules using standard protocols starting from a solution of sodium alginate using calcium chloride ($CaCl_2$) to crosslink the matrix. This produced completely crosslinked alginate capsules of roughly 2 mm diameter. An optical image of the capsules is afterwards reported (see Figure 3.1).

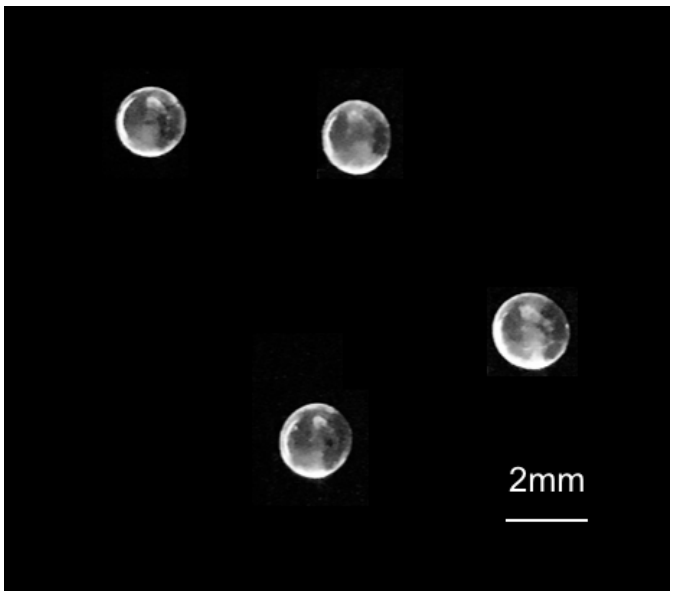

Figure 3.1: **Alginate capsules** Optical image, on black background, of alginate capsules (alginate dissolved in water 5 % w/v) just after crosslinking.

Initial trials showed that the inherent hydrophilicity of the alginate hydrogel was incompatible with the 1-decanol droplet. The capsule created from alginate prepared in water would not stably associate with the droplet and would be shed into the water phase instantly. We then modified the hydrophilicity of the alginate by preparing the hydrogel in water supplemented with varying concentrations of decanoate

surfactant. Capsules prepared with alginate supplemented with 5, 10 or 25 mM decanoate pH 12 showed an increasing association affinity with the decanol droplet. We measured the contact angle of a water droplet (4 μl) on alginate hydrogel formed with increasing concentrations of decanoate surfactant (also at pH 12). After crosslinking the hydrogel surface was washed with *Milli-Q* water and the surface dried briefly using nitrogen gas. We demonstrated the increase in hydrophobicity of the alginate surface with increasing decanoate concentration, as shown in Figure 3.2. The increased hydrophobicity of the alginate allowed for such an alginate capsule (about 1 mm in diameter after drying) to be physically embedded in a 20 μl volume 1-decanol droplet in decanoate solution. Contact angle values are following reported in Figure 3.2.

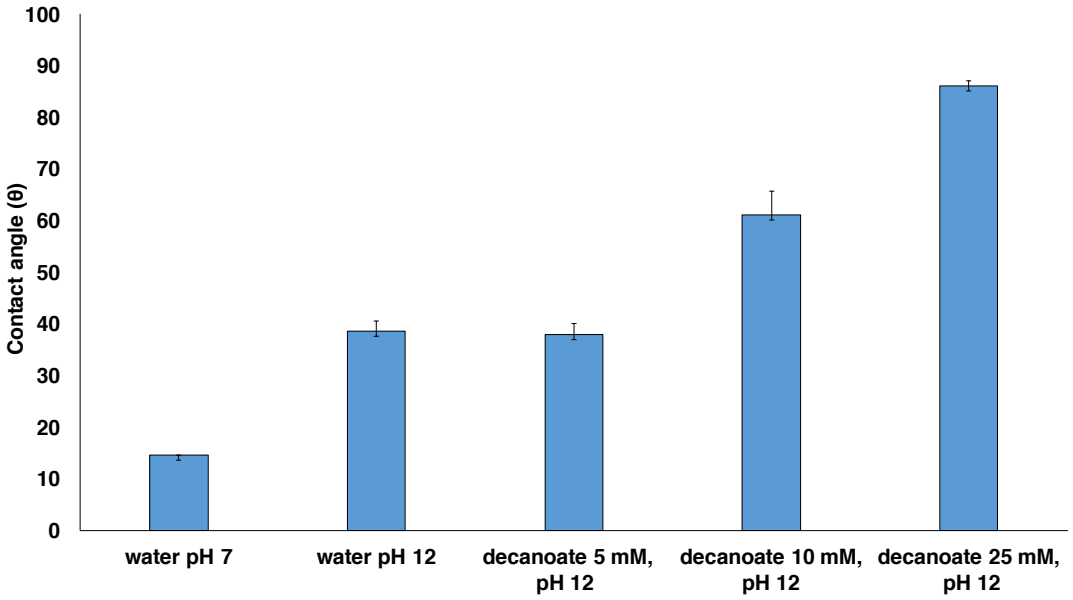

Figure 3.2: **Contact angles of water on alginate hydrogels.** Alginate hydrogel was prepared in various aqueous phases (water pH 7, water pH 12, decanoate 5 mM pH 12, decanoate 10 mM pH 12 and decanoate 25 mM pH 12) and 4 μl of water pH 7 deposited on top. Error bars correspond to standard error on five replicates.

We note that this is a transient surface modification. This is evidenced by long term contact angle experiments that show that pure water droplets on alginate supplemented with decanoate surfactant eventually wet the surface, decreasing the contact angle and indicating that the surfactants ultimately leave the hydrogel interface and distribute throughout the system. Probably, using as 'hydrogel embedded surfactants', surfactants with longer tails would slower this hydrogel modification. In fact as shown in the following chapter, capsules modified from phosphatidylcholine (POPC) show and increased affinity with decanol and a longer attachment to the droplet. However even 'POPC capsules' show this transient modification: loose surfactants at the interface, incorporate water and become to heavy and dense to stay in contact with decanol.

3.1.2 Alginate capsule transport with live cells

Figure 3.3 shows how droplets of 1-decanol can be used to transport and deposit alginate capsules in our system. A capsule of alginate is placed manually inside each droplet of 1-decanol. The droplets

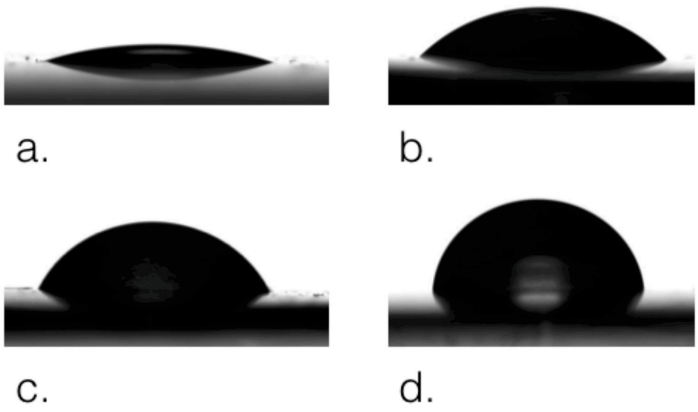

Figure 3.3: **Images of contact angle of water on alginate.** Alginate was dissolved in different aqueous solutions: water pH 7 (a), water pH 12 (b), decanoate 10 mM (c) and decanoate 25 mM (d). The contact angles for the sessile drop of water (pH 7) were as follows: a. water pH 7: $14,5^\circ \pm 1,92^\circ$; b. water pH 12: $38,62^\circ \pm 2,06^\circ$; c. decanoate 10 mM pH 12: $61,02^\circ \pm 2,96^\circ$; d. decanoate 25 mM pH 12: $86,04^\circ \pm 2,01^\circ$. Contact angle value for alginate dissolved in 5 mM decanoate pH 12 was similar to alginate dissolved in water pH 12 ($39,75^\circ \pm 4,6^\circ$).

successfully transport both capsules along the salt gradient. When the droplet reaches the target destination, the alginate capsule cargo is released through the manual addition of a decanoate solution with high molarity (0.2 M). This solution changes the interfacial tension of the droplet and the physical interaction between the droplet and the alginate cargo is disrupted. This allows the cargo to be dropped in a specified position as shown. For a video of this system, see Supplementary Movie 1 25x `https://www.youtube.com/watch?v=zCB2bPhFoCI`.

We see a relationship between the droplet volume and its carrying capacity. For example, a droplet of 10 μl can transport only 1 capsule efficiently. Roughly with an increase of 10 μl in droplet volume, an additional capsule can be stably transported.

3.1.3 Viability of cells after the encapsulation and transport

We tested four different kinds of organisms for encapsulation and transport: three bacteria *E. coli*, *B. subtilis* and *V. fischeri* and one eukaryote, *S. cerevisiae*. To test the sterility of the system, we performed a direct incubation of each organism in 1-decanol oil and in the decanoate aqueous solution, see Methods. Although a few *E. coli* and *B. subtilis* survive for 5 minutes in the 5 mM decanoate solution, none of the organisms survived when placed directly in 1-decanol, confirming the sterility of the system. We tested for the viability of each of the four organisms after being encapsulated inside the alginate capsules and then after capsule transport with the droplet. For encapsulation, the cells were added to the cross-linking step of alginate capsule formation along with their appropriate growth media and the decanoate for modifying the hydrophobic property of the alginate (see Methods). For each organism three replicates of ten such capsules were created, weighed, dissolved and plated on growth media to check for the survival rate of the organisms during the encapsulation step. In addition, individual capsules were added to 1-decanol droplets, transported, released and then harvested for assessment. Three replicates of ten transported capsules were dissolved and serial dilutions were performed for survival assessment and quantification

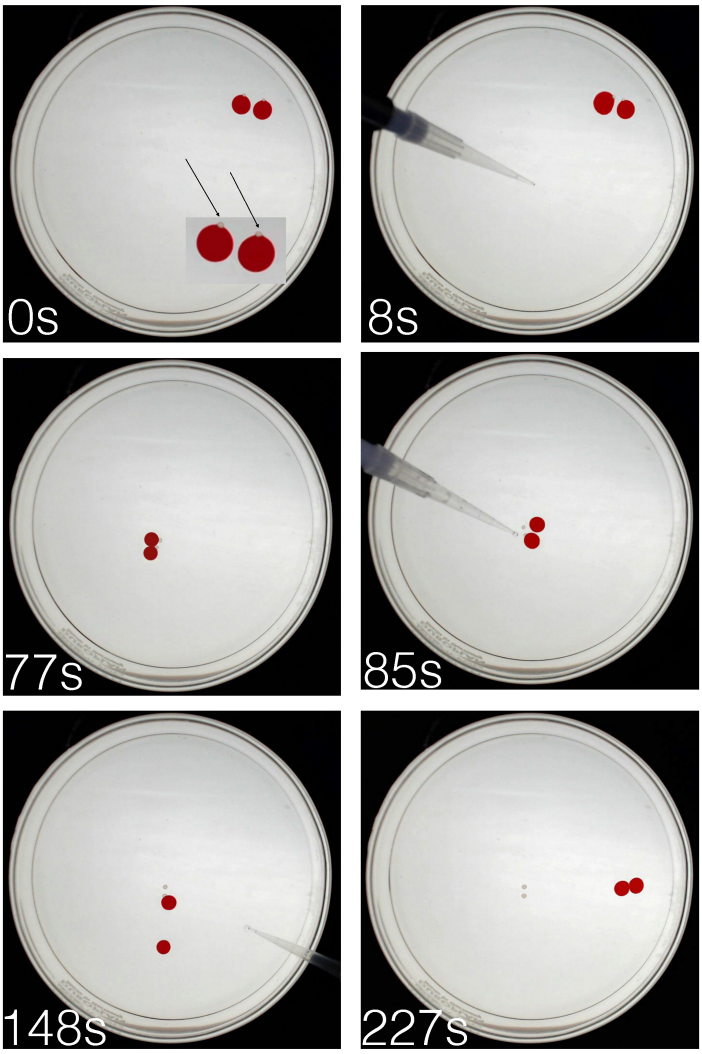

Figure 3.4: **Decanol droplet transport of alginate capsule cargo.** The diameter of the glass Petri dish is 9 cm. Two 1-decanol droplets are placed in the experiment, each containing an alginate capsule of 1 mm diameter (the small capsules are indicated in the inset with arrows). 0 seconds (sec, s): droplets with capsules placed in experiment; 8 sec: salt gradient added with pipette (visible); 77 sec: end of droplet migration towards salt source; 85 sec: 0.2 M decanoate addition by pipette (visible) and capsule deposition; 148 sec: second salt addition; 227 sec: droplet migration towards second salt source. See also Supplementary movie 1.

of the cells. Both *E. coli* and *B. subtilis* survived the encapsulation steps as well as the transport and harvesting step under these conditions (Figure 3.5). Additionally, for visualization purposes, we show that single alginate capsules post transport containing *E. coli* or *B. subtilis*, manually placed on Luria-Bertani (LB) agar plates (Figure 3.5A), showed growth and colony formation.

In contrast we found that both *V. fischeri* and *S. cerevisiae* were more sensitive to such manipulations and did not consistently survive to the end of the transport step. However, we detected that *V. fischeri* survived at least the encapsulation step as evidenced by the autoluminescence test (Figure 3.6).

For yeast, we have confirmed many cases where the cells survive both the encapsulation and droplet-mediated transport. However the survival of the yeast is not consistent even within the same set of replicate experiments and therefore the results are not quantifiable.

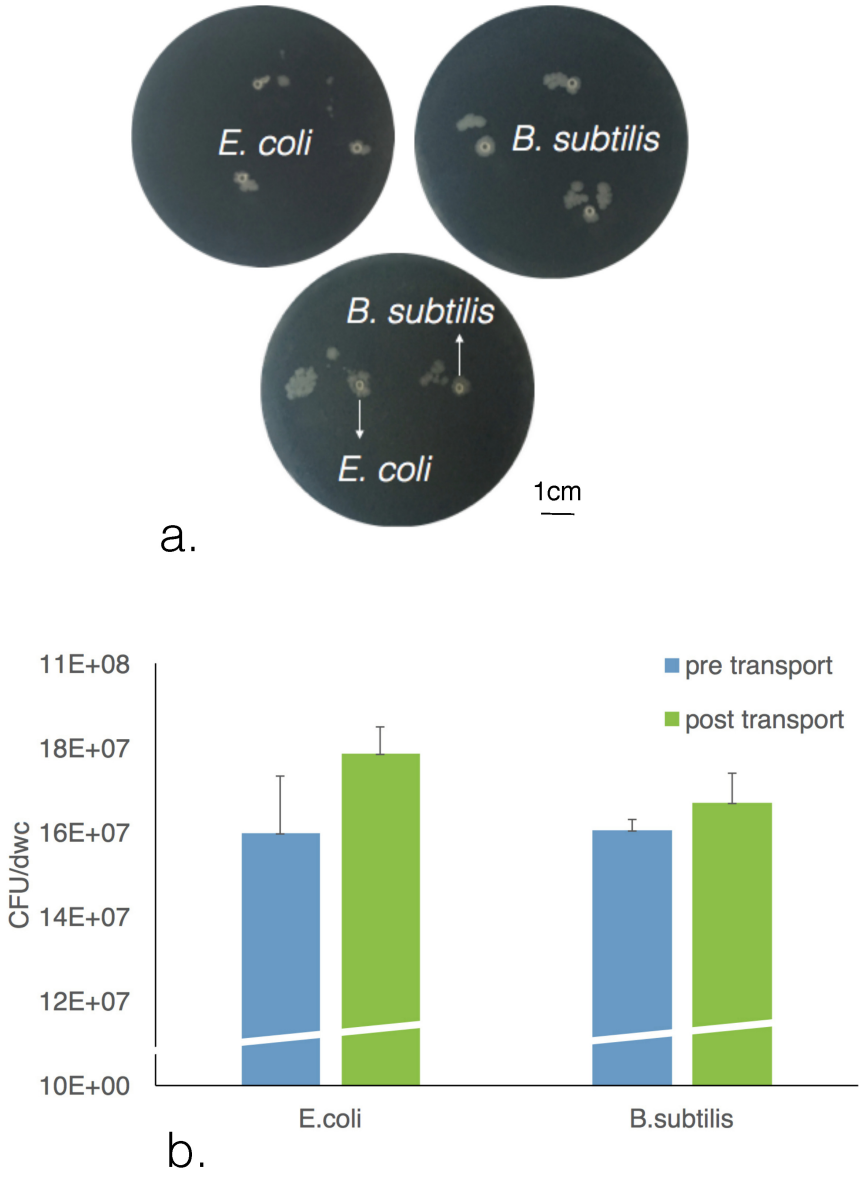

Figure 3.5: **Bacterial encapsulation, transport and survival.** Panel a shows cell growth from transported capsules placed on grown media in Petri dishes. Panel b shows a bar plot that represents the Colony Forming Units (CFU) potential of each of 10 capsules pre and post transport. CFU values are normalized for the dry weight of the capsules (dwc) (error bars correspond to standard errors for experimental triplicates).

Summary of all cell viability assays is found in Table 1.

3.1.4 Confirmation of sterile and aseptic conditions

We confirm that at least two cell types consistently survive both the encapsulation in alginate hydrogel and droplet-mediated transport. To confirm that this system of transport is aseptic and would prevent cell cross-contamination from capsule to capsule or from droplet to droplet within the same environment, we

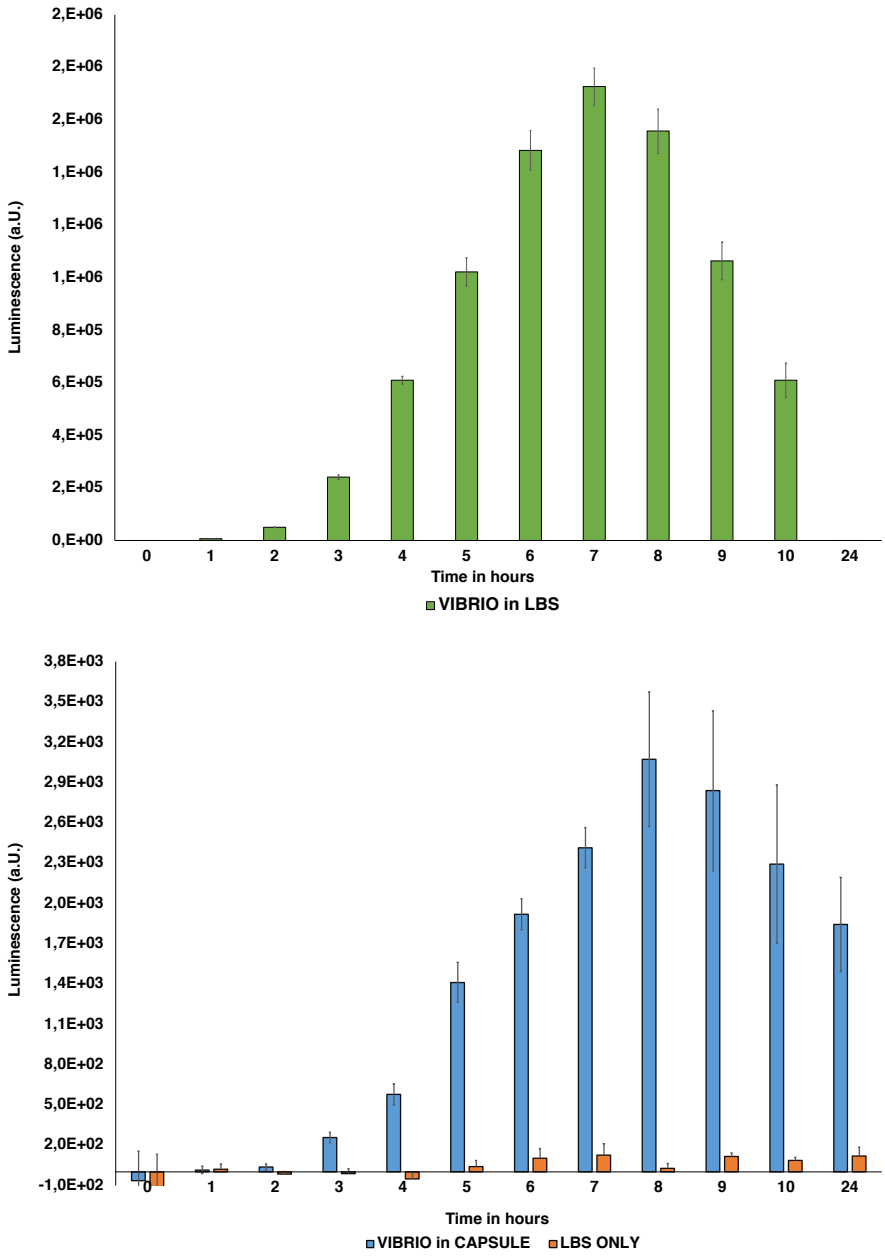

Figure 3.6: **Autoluminescence of *V. fisheri* in alginate capsules.** Luminescence values for *V. fisheri* with or without the alginate capsules over time. Top: luminescence profile over time for *V. fisheri* in LBS without capsule. 100 μl of sample was monitored with a starting O.D. at time 0 of 0.5. Bottom: luminescence profile over time for *V. fisheri* while placed in capsules and LBS alone as a background control. For *V. fisheri* in capsules: 10 μl, 0.2 X of the *V. fischeri* solution at time 0 mixed with alginate dissolved in water 5 % w/v. Time 0 is the time of *V. fischeri* encapsulation. Error bars correspond to standard errors of three technical replicates on three biological replicates of the same kind of sample (VIBRIO in LBS, VIBRIO in CAPSULES and LBS only). All the data were reported in arbitrary units (a.u.) and normalized with the subtraction of luminescence values obtained through the average value of three empty wells.

performed ten transport experiments for each organism (*B. subtilis*, *V. fischeri*, *E. coli* and *S. cerevisiae*). The test involved transporting two capsules per time using two droplets with only one capsule containing

	Direct addition to decanol	Direct addition to decanoate	Encapsulation	Transport
V. fischeri	no growth	no growth	growth	no growth
E. coli	no growth	growth	quantified growth	quantified growth
B. subtilis	no growth	growth	quantified growth	quantified growth
S. cerevisiae	no growth	no growth	growth	growth
Capsule only (control)	no growth	no growth	no growth	no growth

Table 3.1: Summary of cell viability tests

cells. The capsules not hosting cells however did contain the appropriate growth media. The capsules with and without cells were transported as described in the same experiment. After transport, each alginate capsule was harvested and placed in a falcon tube containing 5 ml of fresh media. The alginate hydrogel capsules spontaneously dissolve under these conditions. Following overnight incubation, only the tubes in which capsules containing cells were placed showed any cell growth.

In addition, each solution was spread on specific selective growth plates and only samples derived from capsules originally containing cells showed colony formation. We note that *E. coli*, *B. subtilis* and even *S. cerevisiae* consistently survived the experiment. All controls from capsules containing growth media but no cells showed no growth after transport. Therefore cross-capsule and cross-droplet contamination was prevented under these aseptic conditions. Results of all sterility, cross-contamination, and viability tests are summarized in Table 1 with control capsules labeled as 'Capsule only'.

3.2 Discussion

We have shown an integration of an artificial chemotactic droplet system with the directional transport of living cells. Since the chemotactic droplet system itself is functional under conditions that are incompatible with the viability of cells, a hosting capsule was developed that provided a favorable environment for the cells. In addition the alginate hydrogel capsule supplemented with decanoate surfactant was able to interface with the droplet system, did not disrupt the droplet dynamics, was implantable and retrievable, and was able to release the live cell cargo for analysis and proliferation.

The droplet containing a capsule with live cargo could be manipulated with salt gradients several times with the capsule remaining stably attached to the droplet. In addition, several capsules can be stably fixed to a single decanol droplet. However, capsules placed in the droplet without drying or capsules larger than 1.5 mm in diameter tend to be dropped by the droplet during transport. This is presumably due to high water content of such capsules. Therefore the capsule size more than the capsule number is a limitation of the system.

Once the living cells are introduced to the system, they are subject to several steps of manipulation which could result in cell death: crosslinking in alginate with decanoate surfactant, drying of the capsules over time, placement in the toxic 1-decanol droplet, transport of the droplet with capsule over the course of minutes, release of the capsule from the droplet with additional surfactant, manual retrieval of the capsule from the system, and dissolution of the alginate capsule in fresh growth media. We therefore tested for cell viability at two key steps: after encapsulation and after transport, see Figure 3.5 and Table 1. The best results were with *B. subtilis* and *E. coli* encapsulation and transport. These findings were reproducible and consistent. We see consistent viability of *V. fischeri* in the surfactant-alginate capsules due to detection of their quorum-sensing autoluminescence, see Figure 3.6. However, these cells do not consistently survive the recovery after encapsulation. Additionally we had mixed success with *S. cerevisiae* which survive encapsulation but do not consistently survive transport. Although we follow the protocol strictly and often perform many replicates (up to 10 per experimental condition, see Methods), there is some inherent noise in the system when transporting yeast that is not yet controlled. We therefore will investigate alternative encapsulation methods, such as those mentioned in the Introduction, to allow consistent viability of transported cells including yeast and other eukaryotic cells.

This type of system is presented for the first time and is a proof of principle demonstration including system dynamics and limitations. This represents an alternative platform to live cell manipulation using microfluidics [54]. In our case we take advantage of an open system that can be manipulated easily by hand but also using a robotic interface [55]. The structurally heavy architecture typically used in microfluidic systems for control is not strictly necessary when the actuation of the fluids is performed by the fluids themselves due to dynamic sensory-motor coupling [36]. Therefore such systems could be developed and applied to real world complex environments for the directed motion and delivery of cargo without the need for microfluidic superstructures and support systems. This proof-of-concept demonstration can be further developed for the transport of live cargo due to other controlling signals such as pH [33], heat and light [56]. Transportation of cargo such as organisms or chemicals from one environment to another can also have wider applications. For example, a sulphur-reducing microbial community produces electroactive metabolites such as thiosulphate and hydrogen sulphide [57] and in some cases, all the way to elemental sulphur [58]. These electroactive metabolites can be transported from the sulphur-contaminated environment to a non-contaminated environment and stored. Under the

right conditions, this chemical energy can be converted to electrical energy [57] and so in a way this transport system can result in a new selective energy storage technology. We are currently developing this system towards these targeted outcomes. For example, we are developing a system for droplet mediated cargo transport under physiological conditions which will expand greatly the potential applications of fluid droplet based transport.

3.3 Materials and methods

Materials

All reagents for the chemotaxis experiments were supplied by Sigma Aldrich: decanoic acid, 1-decanol, Oil red O, sodium hydroxide, sodium chloride, sodium alginate, LB broth, agar, yeast extract, peptone and dextrose. Glass DURAN Petri dishes were supplied by Fisher, syringes from PIC and Glass slides from Prestige.

Methods

Unless otherwise specified, experiments were carried out at room temperature.

3.3.1 Surface tension measurement

1-decanol inverted pendant drop surface tension was analysed inside different water phases: decanoate 5 mM pH 11.5 and decanoate 5 mM pH 11.5 mixed 1:1 with NaCl 1, 3, or 5 M. Data were obtained for ten droplets (of 4-5 μl) for each condition using a hooked needle (gauge 22), Theta-lite tensiometer Attension by Biolin Scientific (Nordtest Srl, Italy) and a high precision cell with optical path of 10 mm by Hellmark analytics.

3.3.2 Alginate hydrogel and capsule formation

Alginate hydrogel for contact angle analysis was first prepared with water or varying amounts of decanoate solution at pH 12. Sodium alginate was dissolved (5% w/v) in water (pH 7), water (pH 12, adjusted with 3 M NaOH), or decanoate solution (5, 10, 25 mM at pH 12, adjusted with 3 M NaOH). 1 ml of hydrogel with or without additional surfactant was placed on a glass slide (Prestige Micro slides 26 $\times$ 76m), crosslinked with 1% w/v $CaCl_2$ for 5 minutes and dried briefly with a stream of nitrogen gas. Pure water was then placed on the hydrogel and the contact angle measured for five droplets (of 4 μl) for each condition using a Theta-lite tensiometer Attension, Biolin Scientific (Nordtest Srl, Italy). In parallel with the contact angle experiments, we prepared alginate capsules of roughly 2 mm diameter by crosslinking either alginate in water or alginate in the above surfactant solutions with 1% w/v $CaCl_2$ (see Supplementary Figure S2). Capsule size depends on the dimensions of the needle used for the pre crosslinking extrusion. We tested different types of needles and empirically determined that the 25 gauge, 16 mm needle produced the most consistent spheroidal alginate capsules of the desired diameter. These capsules were dried, using nitrogen gas flush for 5 minutes, dehydrated at room temperature for 3 hours, and then tested empirically for their association with a droplet of 1-decanol (20 μl). After it was determined that alginate supplemented with 25 mM decanoate associated most stably with the decanol droplet and alginate capsules for transport were prepared. Sodium alginate (5% w/v) was dissolved in a decanoate solution (25 mM at pH 12, adjusted with 3 M NaOH). Cells to be transported were grown to a specific optical density (O.D.) and then pelleted and resuspended in fresh medium to a concentrated volume of roughly 1:10 (centrifugation: 1500 rpm 2 min for *S. cerevisiae*, 10000 rpm 10 min for *V. fischeri* and 15000 rpm 5 min for *B. subtilis* and *E. coli*). Nanodrop ND 2000 by Thermo Fisher was used to analyze optical density. The concentrated cells were then mixed with the alginate-decanoate solution (1:5 v/v). The alginate solution containing cells was loaded into a syringe (10 ml, needle 25

gauge, 16 mm) and dropped slowly by hand into 1% w/v $CaCl_2$ for cross-linking. Round capsules were instantaneously formed. The capsules were cross-linked for five minutes and then washed once using *Milli-Q* water. Nitrogen gas was then flushed over the capsules for five minutes. Capsules were at this point consistent with typical alginate hydrogel crosslinked with $CaCl_2$. We note that the outer surface of the capsule became more stiff after drying and capsules had an average diameter of 2 mm. Figure 3.1 shows four alginate capsules with 2mm mean diameter on a black background. Optical image was taken using an iphone SE camera. The capsules were afterwards left to dry for three hours in an incubator at the temperature required for the growth of the organism encapsulated. The drying step was necessary to allow for surfactant assembly at the hydrogel surface to ensure consistent physical association between the alginate capsule and the decanol droplet. After this drying step, the average diameter of the capsules was 1 mm. After drying, the capsules were ready for transport. For capsules prepared without cells as controls, the same procedure was followed except instead of pelleted cells added to the alginate mixture, fresh sterile growth media was added. For capsules containing live cells, the system was prepared as follows: *Escherichia coli* (expressing pEGFP-N1) was taken from glycerol stock and grown overnight at 37°C in LB broth. The same was done for *Bacillus subtilis* 168 strain. *Aliivibrio fischeri* MJ11 was resuspended in Luria-Bertani salt medium (LBS) and *Saccharomyces cerevisiae* BY4741 was instead resuspended in Yeast Extract–Peptone–Dextrose (YPD) and grown overnight at 30°C. Before the encapsulation, the yeast strain BY4741 was diluted and reincubated for three hours to avoid the plateau of yeast growth. *V. fischeri* was instead resuspended in LB until O.D. 0.5. The grown cells were centrifuged and the pellets resuspended in fresh media to a concentrated volume of 1:10 for all four organisms. The obtained mixes were added to alginate 5%, mixed and capsules were prepared, as above.

Droplet-mediated alginate capsule transport Glass Petri dishes of 9 cm diameter were filled with a volume of 9 ml 5 mM decanoate solution pH 11 (adjusted with 3 M sodium hydroxide (NaOH)). Droplets of (20 μl) 1-Decanol were manually added to the system. Then dehydrated alginate capsules were placed manually on the decanol droplets. The chemotactic movement of the droplets was obtained through 3 M sodium chloride (NaCl) addition of 450 μl, as previously described in Cejkova *et al.* 2016 [9]. Alginate capsule deposition was done though the addition of a decanoate solution (300 μl) with a higher molarity (0.2 M pH 12) near the droplet. Droplets were then moved a second time through the addition of 600 μl NaCl. Capsules were retrieved from the system using tweezers and further analyzed, as detailed below.

3.3.3 Cell viability

For assessing the viability of cells after encapsulation but before the transport, 3 biological replicates of 10 alginate capsules were created for each cell culture, dried and dissolved using sodium isocitrate 50 mM solution under continuous shaking for 15 minutes. The recovered samples were then centrifuged (1500 rpm 2 min for *S. cerevisiae*, 10000 rpm 10 min for *V. fischeri* and 15000 rpm 5 min for *B. subtilis* and *E.coli*). The pellets were resuspended in 1 ml growth media, plated after serial dilution (100 μl, from $1:10$ to $1:10^8$, three plating replicates each dilution) and incubated overnight. The plates were counted for colony forming units (CFU). Transport experiment were afterwards performed again with 3 biological replicates of 10 capsules prepared from the growing cell cultures and transported for an average time of 5 minutes. After transport, the capsules were washed with fresh media, dissolved (using sodium isocitrate 50 mM solution) and centrifuged (as above). Dilutions in appropriate growth media (1 ml) were plated

(100 μl) and CFU counted by eye after growth. For each biological replicate of ten capsules, values for three plating replicas were obtained and plotted in Figure 3.5 B.

To record luminescence and check for *V. fisheri* viability, Tecan Infinite M200 plate reader (luminescence mode) and NUNC 96 multiwell polystyrene white plates were used.

3.3.4 Capsule dry weight

To determine the dry weight of the alginate capsules, 5 replicates of 10 capsules, were created, weighed and left drying for overnight in Petri dishes open to air. 10 capsules were used for each assay to average over the capsule to capsule variation in weight and volume. The day after, each replicate was weighed a second time. The mean ratio of capsule weight reduction before and after drying was 0.05 w/w. For each organism 5, 10 capsules replicates, were analyzed.

3.3.5 Confirmation of sterile and aseptic conditions

To test for cross-contamination of the transport platform, 10 experiments of double transport (a capsule with and a capsule without cells on two different droplets) were performed. After the transport capsules were picked up using a sterile tweezer and placed in 5 ml of fresh medium. The capsules dissolved spontaneously in falcon tubes over few hours and the tubes were monitored for cell growth (exploiting O.D.). In addition the recovered samples were plated on selective agar plates and monitored for growth (CFU formation). As an additional test for sterility, aliquots from overnight cultures of all four organisms were directly incubated in 1-decanol or decanoate (10 μl in 5 ml of decanoate or 1 ml of 1-decanol) for a time period corresponding to a typical transport step (5 minutes). To enable phase separation 4 ml of *Milli-Q* water were added in each falcon tube. Falcon tubes were centrifuged, supernatant discarded, and pellets resuspended in appropriate fresh media. Samples from the media were then plated and visually monitored for growth. *B. subtilis* and *E. coli* were plated on LB agar plates, *S. cerevisiae* on YPD plates and *V. fischeri* on LBS agar plates.

We showed that we can selectively transport in a sterile way capsules containing bacteria and that we could efficiently grow them after transport. We decided to try to expand the system towards more physiological conditions and try to transport different types of eukaryotic cells, including human cells, in the next chapter.

Chapter 4

Transport of eukaryotic cells

It was shown, as described before and in [38], that 1-decanol droplets if placed in a specific tensioactive environment are able to move following a chemotactic gradient and transport with themselves 'cargos' of different nature. In this kind of harsh environment some bacteria are able to survive the transport such as *Escherichia coli* and *Bacillus subtilis*.

We conceived the idea to try to evolve this system to transport even mammalian eukaryotic cells. To do this we needed to evolve the droplet chemotaxis system under conditions more conducive to physiological environments. One main characteristic of the aqueous phase in our droplet systems is to modulate the the surface tension between the droplet (1-decanol) and the water phase. Decanoic acid/decanoate acts as the surface tension modulator and can change its properties due to changes in the local environment such as pH or salt concentration. Since the surface tension of 1-decanol in the decanoate solution decreases after that NaCl chemotactic solution is added to it, this variation in surface tension leads to a chemotactic movement of 1-decanol droplets due to salt concentration.

Previously we used the decanoate aqueous phase at pH 11 as we found that empirically this pH supports the chemotactic movement of the droplet. However pH 11 is far from physiological conditions. I modified the decanoate solution by decreasing the pH of decanoate to 7 (using 1 M HCl addition). Then the 1-decanol droplet was tested for chemotactic movement using salt addition. We found that chemotaxis happened efficiently even at this pH. We then tested the system for mammalian cell compatibility and transport.

A549 are epithelial lung cells derived from a caucasian 58 years old man reported to have, at high population density, abundant lamellar bodies enriched with phosphatidylcholine and disaturated phosphatidylcholine. Phosphatidylcholine is afterwards secreted [59]. The main composition of the membranes of this type of cells and their lamellar bodies was found to be: phosphatidylcholine, phosphatidylethanolamine, sphingomyelin, phosphatidylinositol, phosphatidylglycerol, lyso-bis-phosphatidic acid, lysophosphatidylcholine acid, disaturated phosphatidylcholine, phosphatidylserine and cardiolipin [59].This composition corresponds to the pulmonary surfactant one: 80% phosphatidylcholine (PC), of which dipalmitoyl-PC, palmitoyl-myristoyl-PC and palmitoyl-palmitoleoyl-PC together are 75%, Anionic phosphatidylglycerol and cholesterol are about 10% each, whereas surfactant proteins SP-A to -D comprise 2-5% [60]. Knowing that A549 cells secrete these kinds of substances in their environment, we then wanted to test not only cell transport but if the natural surfactants produced by the cells could substitute for the decanoate 1) in the aqueous phase and 2) in the hydrogel to modify the surface of the alginate.

We tested the eukaryotic cell transport also with two non cancerogenic cell lines: RPE1 and HEK 293 T. RPE1 are epithelial cells of the retina obtained from an healthy woman. HEK 293 T cells are an human embryonic kidney cell line.

4.1 Results

4.1.1 Capsule characterization

The produced capsules have a diameter that varies between 2,5 and 3 mm. Their mean weight is 15,7 $\pm$ 0,6 mg (values obtained from 10 replicates of 10 capsules) with a volume of 15,15 $\%$ μl. Capsule look similar to the ones shown in Figure 3.1 [38].

4.1.2 Droplet chemotaxic transport of A549 cells

As said before, we tried to evolve the droplet chemotaxis system under conditions more conducive to physiological ones. We tried to transport capsules using droplets in decanoate 5 mM pH 11 but even pH 7. Typically when a 1-decanol droplet is added to the aqueous phase, short random movements occur before the chemoattractant is added to the system. We decided to try to reduce these random movements by saturating the decanoate aqueous phase with 1-decanol before conducting the experiment. Decanoate was placed in a glass bottle (500 ml), 10 ml of decanol added to it and solution was saturated 'manually shaking' the bottle in which the two phases were placed, waiting 1 hour for phase separation and pouring away decanol. We then tested the 1-decanol droplet system using the decanoate system saturated with 1-decanol. This treatment largely eliminated the initial random movements. This result indicates that the initial random movements was due to the loss of mass of the 1-decanol in the decanoate solution. It is likely that the soapy decanoate dissolves part of the decanol oil droplet and this loss of mass along part of the interface results in the spurious movement. By eliminating these random movements, the actual chemotactic movements were easier to observe both by eye and through image processing (see Chapter 6).

We tested many other aqueous conditions that could be favorable to the survival of the mammalian cells. One of the main test was for surface tension differences of the aqueous phase in air, compared with pure water (72 mN/m). Using Theta-lite tensiometer by OneAttension, Biolin Scientific (Nordtest Srl, Italy) we checked for the surface tension of decanoate solutions 5 mM (pH 7, pH 7 saturated and pH 11), Dulbecco's Modified Eagle Medium (DMEM) and DMEM in which alginate empty capsules were incubated one or two days. The obtained surface tension values are reported in Figure 4.1. This shows that the surface tension of decanoate 5 mM pH 11 is reduced if compared to the surface tension of water and reduced even more in the case of decanoate 5 mM pH 7 and saturated decanoate 5 mM ph 7. For terminology, we refer to DMEM or DMEM pure as the DMEM freshly obtained from Invitrogen, to DMEM phase or DMEM water phase to the DMEM pure in which the capsules with eukaryotic cells have been incubated for two days and to DMEM complete as DMEM pure with the addition of Penstrep (1 $\%$), L-Glutamine (1 $\%$) and FBS (10 $\%$).

We checked for surface tension reduction even for DMEM water phase in which cell lines were incubated. When the DMEM cell capsule water phase did not show any reduction in surface tension if compared to the one of DMEM alone, we increased the capsule incubation to two days. After two days DMEM water phase showed values of surface tension lower than 70. After 20 minutes of readings by the pendant drop method, the surface tension values were decreased to values between 60 and 55 mN/m.

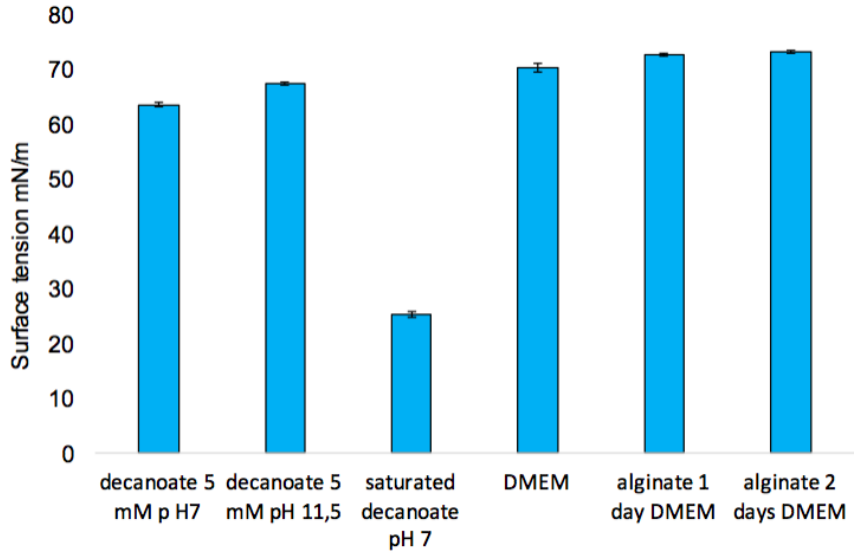

Figure 4.1: **Pendant drop surface tension**

Surface tension of different aqueous phases: decanoate 5 mM pH 11.5, decanoate 5 mM pH 7, saturated decanoate 5 mM pH7, DMEM and alginate one or two days in DMEM. Error bars correspond to standard deviation of 10 replicates.

We better analyzed the capsule water phases using surface tension of inverted pendant drop of 1-decanol inside it. Capsules water phase showed a decrease in surface tension compared to DMEM. Values are reported in Figure 4.2.

A549 capsule transport experiments were performed similarly to bacteria and yeast transport. Transport was performed in decanoate 5 mM pH 7 or in DMEM cell capsules water phase creating a salt gradient using 3 M NaCl. All the capsules were transported and all dissolved and analyzed. In the case of capsule release, drop was obtained using decanoate 0.2 M pH 12. Otherwise capsules were picked up using tweezers.

4.1.3 Chemotaxis using the water phase from capsules with A549 cells

To characterize if the potential surfactants produced by A549 cells could substitute for the decanoate we tested the water phase from A549 cells encapsulated in the capsules, that showed surface tension reduction (see Figure 4.2), in a chemotaxis experiment. After the salt solution addition droplets moved to the source and capsules were deposited using 0,2 M decanoate pH 12. For comparison, we tested for chemotaxis even in pure DMEM, DMEM complete and DMEM in which empty capsules were incubated for two days but without cells added. These water phases did not support droplet chemotaxis. Only water phases in which living A549 cells in capsules were incubated showed the ability to support chemotaxis. This indicates that the living cells under these growth conditions produce surfactants that can fully substitute for the decanoate.

4.1.4 Bi-phase hydrogel modification test

We tested if there was a correlation between the amount of surfactant added during the capsule formation step and the propensity of the capsule to remain associated to the droplet during transport. We devised an easy assay to check for this by preparing a biphasic system. The aqueous phase was placed in wells

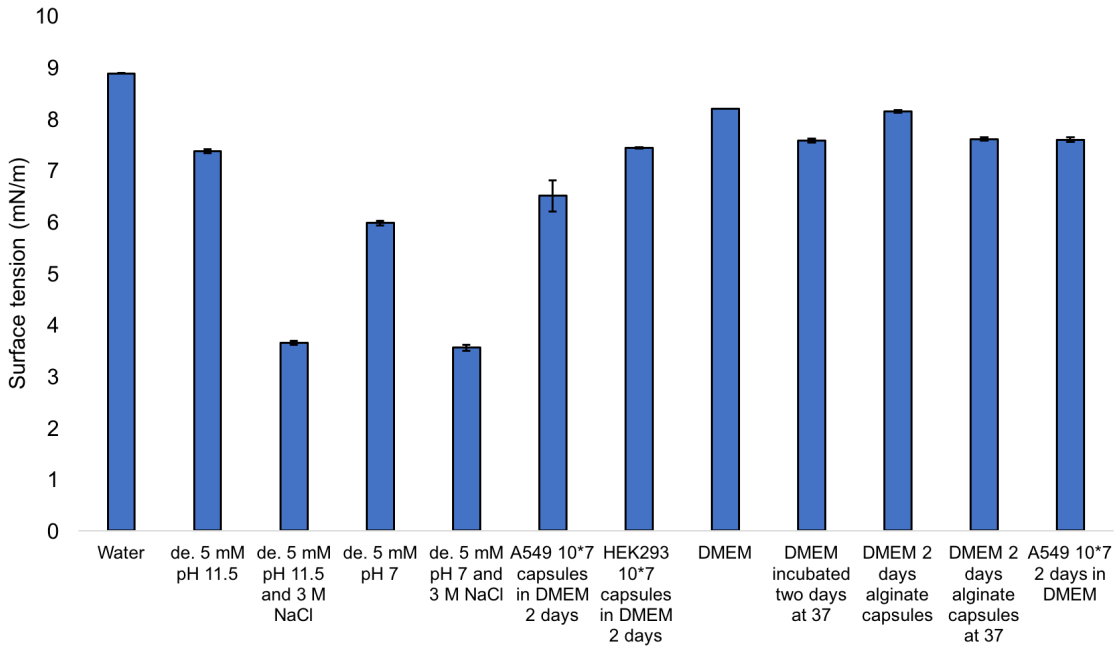

Figure 4.2: **Inverted pendant drop surface tension** Surface tension of 1-decanol in different aqueous phases (de. stands for decanoate). Surface tension (in mN/m) for 1-decanol inverted pendant drop in: water, decanoate 5 mM pH 11.5, decanoate 5 mM pH 11.5 mixed 1:1 with NaCl 3 M, decanoate 5 mM pH 7, DMEM in which 10*7 A549 cells in capsules have been incubated for two days at 37°C, DMEM in which 10*7 HEK293T cells in capsules have been incubated for two days at 37°C, DMEM pure, DMEM Incubated for 2 days at 37°C, DMEM incubated with empty alginate capsules two days at 37°C, DMEM incubated with empty alginate capsules two days at room temperature and DMEM with 10*7 A549 cells incubated 2 days at 37°C. Error bars correspond to standard deviation of 10 replicates.

of a 20 well plate. Then the 1-decanol oil phase was placed on the top. To this biphasic system the capsule prepared in various ways was placed at the oil-water interface. The amount of time that the capsule remained at the interface was recorded. We found that the results of this assessment was in good agreement with the propensity of a capsule to be transported or lost during droplet-mediated transport.

Water phase (DMEM), in which capsules were incubated for two days was poured away, and when mixed with alginate was immediately gelling and producing a material difficult to manipulate. We thought this water phase could have contained some surfactants giving the alginate this property. We resuspended the test water phase in pure water at different ratios (1:1, 1:5, 1:10 and 1:20) and dissolved sodium alginate in them. After crosslinking, the capsules produced from these ratios were manually placed in the biphasic test and the association times recorded (for more details see methods). A table of the time of capsule-interface association can be found in Figure 4.3 for various conditions tested. The values for the association of the capsules dissolved in water phase dissolved 1:1 in water were higher than one hour and not reported in the graph. We can clearly see that water phase contains compounds that highly increase the droplet-capsule affinity and we can use this to tune the association of the capsules with the droplets.

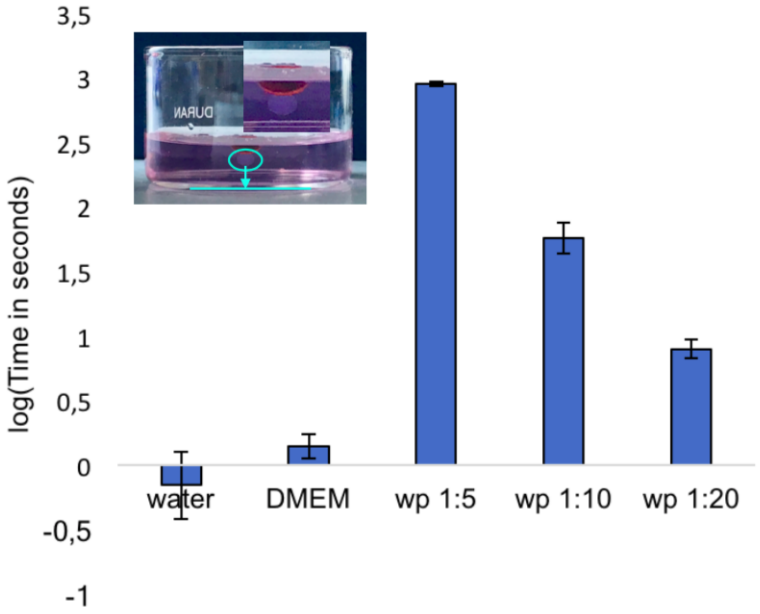

Figure 4.3: **Bi-phase hydrogel modification test** Capsules are prepared dissolving alginate (5% w/v) in different pre-filtered water phases. Capsules are manually placed upon a decanol droplet and the timings of the droplet-capsule association are recorded: water 0,7 ± 0,67 sec; DMEM 1,4 ± 1,3 sec; 1:5 912 ± 107 sec; 1:10 58 ±7 sec; 1:20 8 ± 1 sec. For each condition 10 replicates are performed. By light blue arrow, circle and line in the optical image, the dropping of the capsule as observed is indicated. Dropping is shown in a glass beaker for easier visualization.

4.1.5 Cell survival after transport

As bacterial cells (Chapter 3) mammalian cells were placed in the alginate capsules and transported. The system was then tested for viable cells post-transport. The viability of the cells was tested by trypan blue staining and dissolving and plating all the transported capsules. The amount of cells that we had after the transport was 1:10 reduced if compared to the pre-encapsulation amount. Therefore the majority of the cells were lost. There are many steps of our protocol that could diminish cell number. For example, the release of cells from the edge of capsule during crosslinking and during DMEM incubation, and the cell-alginate mixing and extrusion during which half of the alginate volume is lost The mean viability after the transport in decanoate pH 7 (normal or saturated) of A549 cells in capsules is 40% and after transport using water phase environment of A549 capsules is 80%. If we add the release step using decanoate 0.2 M pH 12 survival rate drops to 20% and 60% respectively. In addition to the transport of A549 cells, we tested the transport of RPE1 and HEK 293 T cells. Both cells lines showed a viability of 20% after encapsulation and none survived transport. We determined that the detrimental step for HEK 293 T and RPE1 survival are the two days of incubation in DMEM. In fact when these cells are incubated in petri dishes in DMEM not complete for two days, they are afterwards not able to proliferate anymore. A549 incubated on petri dishes at 37 degrees and 5% CO_2 with DMEM complete after capsules dissolution in sodium isocitrate seem to still proliferate before transport but not after.

4.1.6 Cell transport autoselection

In addition to testing the transport of living mammalian cells, we wanted to know if such cells could naturally produce surfactants that could replace the decanoate that we artificially add to the aqueous phase or to the alginate crosslinking for surface modification. If so, then perhaps this whole chemotactic cell transport system could act as an 'autoselector' for cells producing surfactants. We tried to incubate and transport not only the capsules with live A549 cells (that produce surfactants) but even with dead A549 and empty capsules (no surfactants). We found out that only the ones with viable A549 are able to be efficiently transported. For both empty capsules and capsules with dead cells, when the capsules are placed on the 1-decanol droplet, they are instantaneously released. We tried to transport each type of capsule 10 times. We checked for cell release from the capsules after two and three days of incubation but cells were under the quantifiable range. And so we supposed almost no cell were released from capsules.

4.1.7 Cells in capsule visualization

Cell are present when the hydrogel capsule is formed. We wanted to visualize the cells inside the capsules. Cell in capsules were visualized using a staining with calcein AM and Propidium Iodide. Calcein AM stains alive cells that will appear in the images green and propidium iodide stains dead cells that will appear red. This live-dead staining was performed on capsules containing A549 cells isolated before and after transport (in A549 capsules water phase) and after the release using 0,2 M decanoate pH 12 (see Figure 4.4). Capsules before and after transport, showed high viability (visualizable by the green color of calcein AM). Cells in the middle of the capsule are not properly stained this due to the high density of the alginate gel. I tried to cut partially a capsule and stain it. Cells were well stained from calcein and alive even inside the capsule. It is possible that the cells inside the capsules were blocked in G0 as they appeared roundish. This might explain why the cells are not able to proliferate properly after transport.

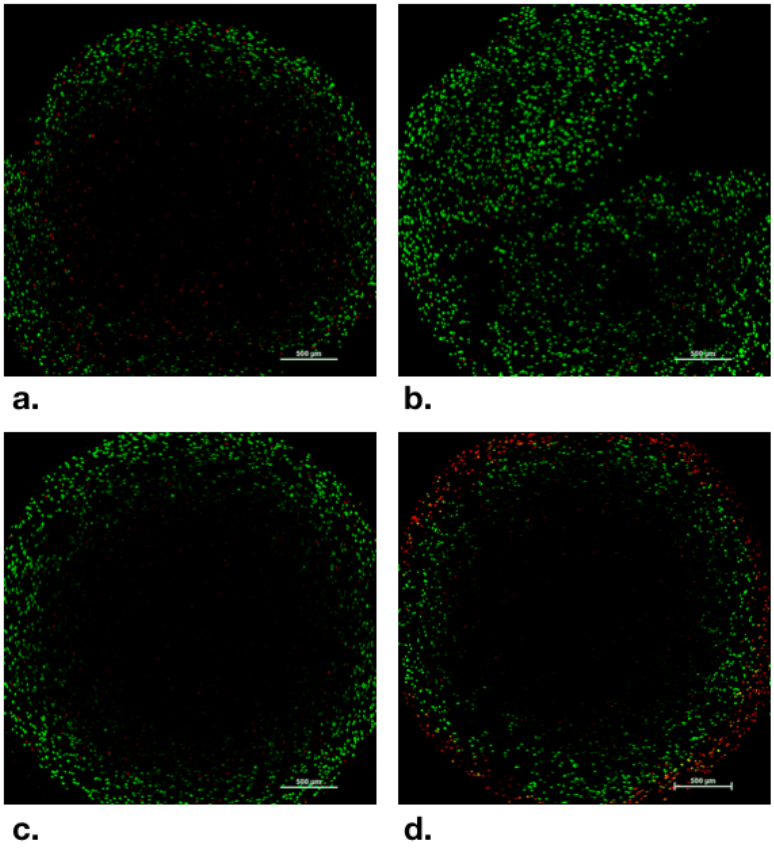

Figure 4.4: **Live-dead capsules staining**

Calcein AM (green) and PI (red) staining of: a. capsules pre transport, b. cut capsule pre transport to let the staining penetrate, c. capsule post transport and d. capsule after using 0.2 M decanoate pH 12 to drop the capsule cargo.

4.2 Discussion

As with the droplet-mediated transport of bacterial cells in Chapter 3, we wanted to test if our system could be compatible with and transport human cells. In addition we wanted to know if naturally produced surfactants could substitute for the decanoate we normally add to our experiments. We found that A549 cells can be encapsulated in alginate hydrogels and they are alive. When in capsules incubated in DMEM, the cells survive and secrete into their environment some compounds that lower the surface tension and act as surfactants. Such compounds could be similar to the components of lamellar bodies: phosphatidylcholine and disaturated phosphatidylcholine. The water phase in which capsules are incubated shows a reduction in surface tension if compared to water and can be used as chemotactic water phase. Some of the molecules secreted by the cells seem to get trapped inside the alginate borders of the capsule and modify the surface of the capsule itself. The surface becomes able to associate efficiently and for a long time with 1-decanol droplets (up to 1 hour in the case of water phase mixed 1:1 with water). The capsule can be transported, using chemical gradient in a specific location and dropped thought the addition of a high surfactant content water phase. After the transport A549 cells seem still alive but not proliferating anymore. If in fact plated before the transport they are still able to proliferate, but seem blocked in G0 (round morphology and not proliferating) if plated after transport. The same G0 like block is seen even for A549 cells simply plated in DMEM for few days. If DMEM is afterwards taken away and

DMEM complete substituted instead, they proliferate again. We tried to transport also two other types of non cancerogenic cells: HEK 293 T and RPE1. They do not survive the encapsulation or the transport. Using the surface tension analysis and the biphasic association tests, we also determined that they do not secrete surfactants under these conditions. These two types of cells already show a problems even when incubated in DMEM, they in fact do not proliferate anymore and die after only two days of incubation. The addition to DMEM was found as the step that causes these two cell lines to be non-viable. DMEM incubation is however needed to have comparable results of water phase surface tension. Surface tension of DMEM complete is reduced if compared to DMEM. DMEM complete however does not work as a chemotaxis water phase as A549 cell capsule DMEM does. The surface tension reduction in DMEM complete is probably due to not tensioactive compounds that should be instead present in pure DMEM in which capsules with cells are incubated for two days.

1-decanol is toxic to A549 cells [62]. Therefore A549 cells do not proliferate after transport and exposure to the decanol. We can hypothesize that if we will be able to find a cell line that has no problems proliferating in DMEM and without problems of toxicity for 1-decanol we would have a system able to transport eukaryotic cells efficiently and in an auto-selective way. We have found out that the A549 water phase contains compounds that allow for high affinity of the hydrogel with 1-decanol droplets. This water phase could be exploited to dissolve alginate, produce highly decanol affinity capsules and also act as a new chemotaxis environment in which new oil phases could show chemotaxis.

4.3 Materials and Methods

Materials

All reagents for the chemotaxis experiments were supplied by Sigma Aldrich: decanoic acid, 1-decanol, Oil red O, sodium hydroxide, sodium chloride and sodium alginate. Glass DURAN Petri dishes were supplied by Fisher and syringes from PIC. DMEM complete 1x and Trypan blue dye were provided by Invitrogen.

Methods

Unless otherwise specified, experiments were carried out at room temperature.

4.3.1 Alginate hydrogel and capsule formation

Alginate capsules for transport were prepared by first dissolving sodium alginate (5 % w/v) in *milliQ* filtered water. Cells to be transported were grown until 80% confluence in DMEM complete (DMEM high glucose with the addition of 1% Penstrep, 1% L-Glutamine and 5% FBS), resuspended, counted and viability was checked. Cells were then pelleted and resuspended in fresh DMEM to a final concentration of 2x10*7 cells for 1 ml (centrifugation: 1500 rpm 5 min). 1 ml of cell resuspension was mixed with 5 ml of sodium alginate gel. The alginate mix was loaded into a syringe (needle 25 G x 5/8", 0.50 $\times$ 16 mm) and dropped slowly by hand into 1% w/v $CaCl_2$ for cross-linking. The capsules were cross-linked for five minutes, washed once using DMEM and incubated for two days in DMEM (37° and 5% CO_2). After drying for 30 minutes inside the biological hood, capsules were ready for transport. This procedure was followed even for capsules containing dead cells (autoclaved) and empty ones (no cells added). With

the only exception that for control capsules instead of adding pelleted cells to the alginate mixture, fresh sterile growth media was added.

4.3.2 Transport and cell viability assessment

Petri dishes were filled with decanoate 5 mM pH 7 solution or A549 water phase (mixed 1:1 with water). Capsules were dropped on 1-decanol and transported through the creation of a salt gradient [38]. In the case of drop capsules were released using decanoate 0,2 M pH 12. Cells were counted and viability checked before and after transport. To assess them, capsules were washed with DMEM, dissolved using 50 mM sodium isocitrate (shaking incubation) for 15 minutes, centrifuged, pelleted and resuspended in 100 μl PBS. Cells and their viability were quantified using trypan blue dye, countess cell counting chamber slides by Life Technologies and countess automated cell counter by Invitrogen.

4.3.3 Surface tension of the chemotaxis water phase

Using Theta-lite tensiometer by OneAttension, Biolin Scientific (Nordtest Srl, Italy) we checked for the surface tension of pendant drop water phase after one or two days of incubation. As soon as the surface tension decreased inverted pendant drop surface tension of 1-decanol inside the water phase was measured. For each condition ten 1-decanol drops were analyzed.

4.3.4 Bi-phase hydrogel modification test

The water phase obtained from the capsule incubation is filtered using 0,22 μm filters in PES (by Euroclone) and mixed with water in different quantities: 1:1, 1:5, 1:10 and 1:20. Sodium alginate is dissolved in these solutions at 5 $\%$ w/v. An homogeneous gel is obtained through magnetic stirring and afterwards cross-linked in 1 $\%$ w/v $CaCl_2$. The obtained capsules are dried for 30 minutes under the biological hood and ready for the affinity test. Each well of a 20 well plate dish is filled with 1ml of capsules water phase and 200 μl of 1-decanol added it. Capsules are manually placed, using tweezers, upon the decanol droplet (30 μl) and the time needed for them to be drop to the bottom of the well plate recorded.

4.3.5 A549 auto-selectivity test

Three types of capsules were transported: capsules with A549 cells, empty capsules (no cells) and capsules containing autoclaved dead A549 cells. Capsules were created using the previously described protocol. For empty capsules fresh DMEM was added to the alginate solution. For dead cells, the cells were counted, taken in the same amount of live ones, autoclaved, pelleted, resuspended in fresh DMEM and mixed with alginate. After 2 days of incubation in DMEM capsules were ready for transport and the 'water phases', in which capsules were incubated ready for further analysis.

4.3.6 Capsule staining

Capsules were taken at three different time points (after cross-linking, after 2 days of incubation and after transport) and incubated in Calcein AM and propidium iodide staining solution (1:1000 and 1:500) for 1 hour. Capsules were afterwards visualized at the confocal microscope.

We showed in this chapter new perspectives for transport and growth of eukaryotic cells. We developed our chemotaxis systems towards conditions more conducive to physiological ones, had cells that seemed still alive after transport and blocked with 1-decanol their cancerogenic potential. There are other types of biological multicellular system with which would be interesting to study the integration and effects of our chemotaxis system. In the next chapter we will explore the 1-decanol system effects on biofilms on ceramic tiles and membranes inside microbial fuel cells.

Chapter 5

Integration of chemotactic droplets with living biofilm

All my work was part of the FP7 European Project: EVOBLISS. In accordance with the overall goals of the EVOBLISS project, we strive to integrate our artificial chemical life technologies with living systems to affect them in a positive way. We tried not simply to integrate droplet with capsules containing our biological entities, cells, but even to integrate droplets in a collaborative way with Microbial Fuel Cells (MFCs). This part of work was performed in my exchange period at Karlsruhe Institute of Technologie (KIT). Our collaborators at KIT helped me with the optical coherent tomography (OCT) images and the voltage output recordings on MFCs.

Our targets were to interface with biological systems, to spatially and temporally control the introduction of impregnated droplets into living biofilms and to affect the behavior or output of the living system. We have approached this target using two chemical systems: a) chemical droplets that have the potentiality for movement and chemotaxis b) alginate droplets or capsules that can even be transported by the droplet itself.

5.1 Microbial fuel cells

The microbial fuel cell (MFC) technology has captured the attention of the scientific community in the last decade for the possibility to transform organic waste into electricity using microbial catabolism. The idea of MFC was conceived by Potter in 1911 [63]. Conceptually, a microbial fuel cell consists of two chambers, the cathode and the anode chamber, separated by a membrane. The anode is where nutrients or organic waste and bacteria are placed. In the anode, the bacteria oxidize the waste products and release electrons that are transferred to the cathode [64]. We had two groups in our european project working on MFCs, KIT and University of the West of England (Iorepoulos group). They had two differential settings of MFCs: horizontal and vertical respectively. Ioerepoulos et al. created in 2003 EcoBot I, a robot directly powered from MFCs [65] and able to move photo-tactically and it evolved for two generations until the creation in 2013 of EcoBot III [66]. For our European Project EVOBLISS a key question was how microbes colonize a microbial fuel cell, what structure the biofilm had and how this structure is likely to influence the performance of the microbial fuel cell. In EVOBLISS, Karlsruhe Institute of Technology in Germany is responsible for this part of work and uses advanced three-dimensional OCT scanners to

sample living microbial fuel cell and the work performed with them for droplet integration in MFCs is following described.

5.2 Results

5.2.1 Biofilm and droplet interaction

Biofilm cultivation was performed on ceramic tiles of size 4 cm x 4 cm for approximately 30 days. The tiles were placed in a fume with low COD concentrations to mimic biofilm growth in a natural environment, such as rivers. After sufficient biofilm growth, the ceramic tiles were provided me from KIT and I transferred them from the fume into a petri dish containing 5 mM decanoate solution of pH 11.

A chemical droplet of 20μl 1-decanol with or without Oil Red O was added and the biofilm (and droplet) were imaged with the OCT. Figure 5.1 A shows the decanol droplet (with Oil Red O colorant) in the biofilm. Figure 5.1 B shows a single cross-sectional image from the OCT scanning of the system. The OCT was able not only to image the biofilm but also the position of the droplet due to the refractive index (see `https://youtube/24pvYhTqcc8`). During the course of the observation, no change in biofilm structure was observed due to the presence or movement of the droplet.

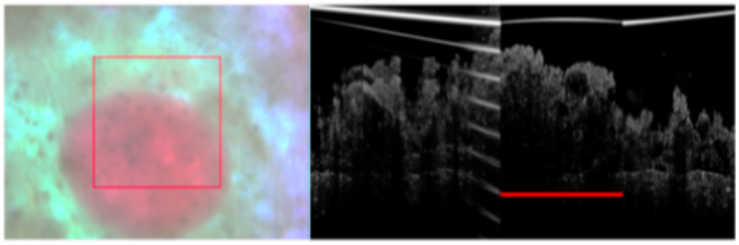

Figure 5.1: **A droplet of decanol in a system containing living biofilm** A, optical image of a 1-decanol with Oil Red O as colorant added to a living biofilm. The area outlined in the red square was imaged over time with the OCT. B, cross- sectional image from OCT scan of a 1-decanol droplet moving above the living biofilm. No dye was used. The red line marks the diameter of the droplet for clarity. The dimensions of the cross sections were: 5 mm x 1.95 mm (1024 px x 700 px) with a resolution of dx = 4.88 μm and dz = 2.79 μm. Follow video link: `https://youtube/24pvYhTqcc8`

To test for droplet chemotactic function in the presence of biofilms, a ceramic tile was placed into a petri dish with 5 mM decanoate solution pH 11 added, as before. A chemical droplet of 20 μl 1-decanol with Oil Red O was added to the edge of the system and then a chemical salt gradient was used to induce chemotactic movement across the biofilm. The droplet was able to sense and to move under these conditions (Figure 5.2) but with considerable difficulty as the droplet movement was physically hampered by the biofilm (see `https://youtu.be/ir9BYkC4T-Q`). Afterwards we did not detect any change in the biofilm structure as the result of the droplet position or path. However, after 28 days a general deterioration of the biofilm was apparent under these conditions (Figure 5.3).

Previously, they tested at KIT the effects of the presence of 1-decanol and a pre-known harmful compound (chloroform) on the power output of the biofilms growing in MFCs. 6-8 ml of this two compounds were added to working MFCs, covering the biofilm on the anode side, and the voltage output was monitored over time. As Figure 5.4 shows, the presence of the decanol did not appear to affect the

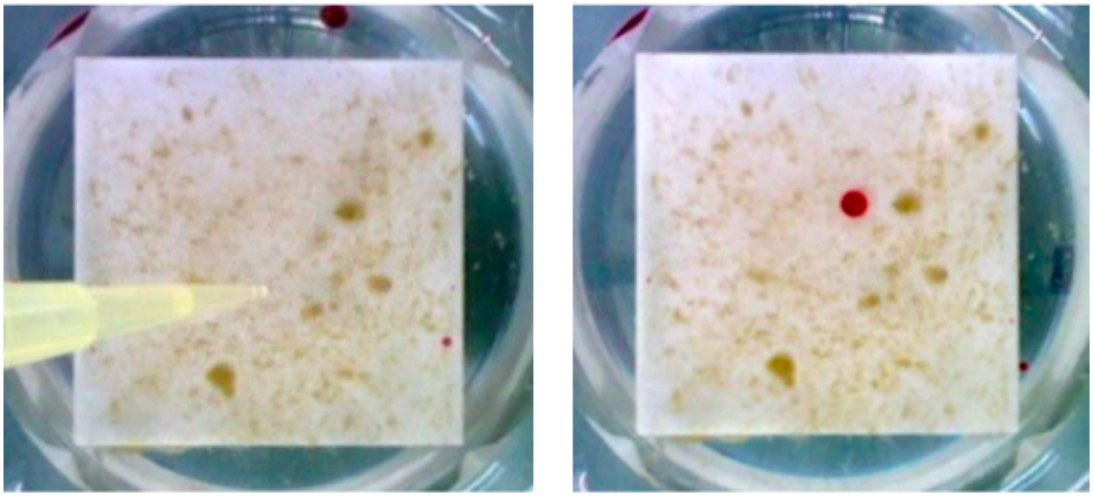

Figure 5.2: **The chemotaxis of decanol droplet over the biofilm surface.** A – starting position: red droplet at top of image, B – movement of droplet across biofilm. Ceramic tile size: 4 cm x 4 cm.

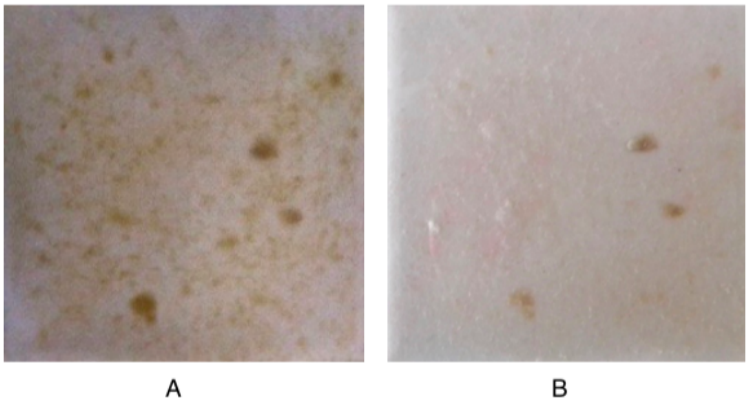

Figure 5.3: **The chemical degradation of the biofilm caused by the incubation in decanoate solution.** A – the first day of incubation, B – 28th day of incubation. Ceramic tile size: 4 cm x 4 cm. D3.3.2 MFC output and droplets

output of the MFC over the time monitored. Whereas the presence of the chloroform gradually reduced the output of the MFC. This represents a poisoning of the biofilm and points to the lack of bio-compatibility of some of our chemical systems with living systems. Thus results obtained at KIT confirmed the 1-decanol non toxic nature in MCFs.

5.2.2 Alginate and biofilms

Since we detected either no effect (decanol) or negative affect (chloroform or decanoate solution) of chemical droplets on the biofilm, I performed some experiments with alginate, that we assumed would be more bio-compatible.

Alginate capsules were prepared by dissolving sodium alginate (3% w/v) in tap water. Two types of capsules were prepared, containing different concentrations of glucose, extruded and cross-linked in

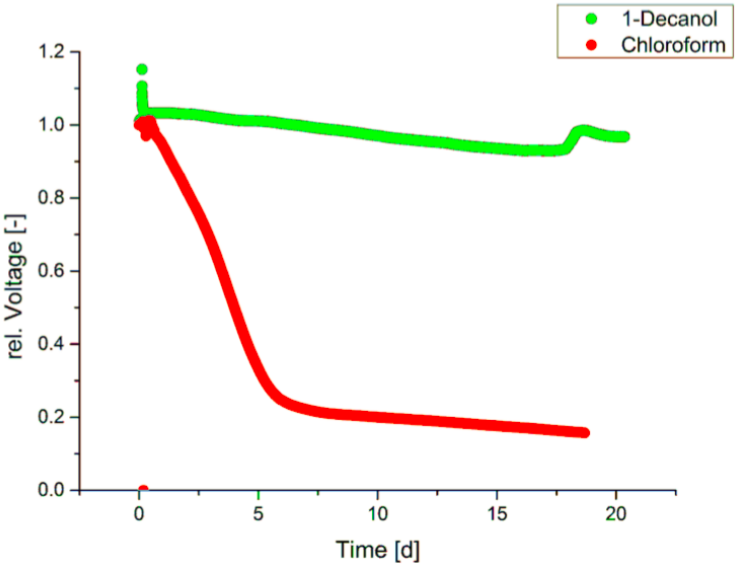

Figure 5.4: **MFCs output** Graph showing the decrease in output of the MFC with chloroform added (red line) and the stable output of added decanol (green line).

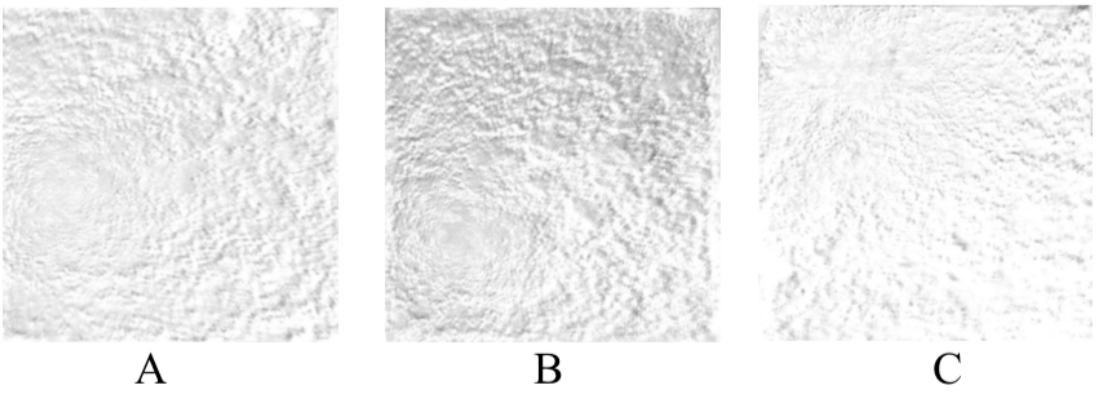

Figure 5.5: **Optical image subtraction of day 5 from day 0.** A biofilm incubated with 0.1% w/v glucose in alginate, B biofilm incubated with 1% w/v glucose in alginate; C control biofilm incubated without capsules.

calcium chloride (CaCl2) 1% w/v solution. The capsules were dehydrated were placed on the surface of biofilm growing on ceramic tiles. Biofilms were then covered with a layer of tap water. For the first five days of the experiment, each sample was supplied with 10 ml of 0.1 M sodium citrate solution at 1-day intervals as a potential nutrient but also to chelate the calcium ions and slowly dissolve the alginate capsules. This releases the stored glucose inducing further biofilm growth. On the sixth day, tap water and the residuals of dissolved capsules were removed and optical images of the biofilms were taken using a Nikon camera. The images were then processed, using Fiji software. The blue color channel of the image, showing the highest sensitivity for biofilm, was selected and inverted to perform the analysis. The image analysis revealed that introducing alginate capsules impregnated with glucose resulted in increased growth of the biofilm, as expected (Figure 5.5 A and B). The images represent the amount of biomass increase over five days. The darker the image, the more biofilm formed, with the higher amount of glucose

inducing the most growth (Figure 5.5 B). The sodium citrate control (Figure 5.5 C) revealed the negligible effect of sodium citrate on the growth of biofilm in the experimental period of 5 days. Note that using this standard analysis technique it is not possible to provide a quantitative measurement of the amount of biofilm rather it is used to observe qualitative difference.

5.2.3 Spatially and temporally controlled induction of the living system using alginate capsules

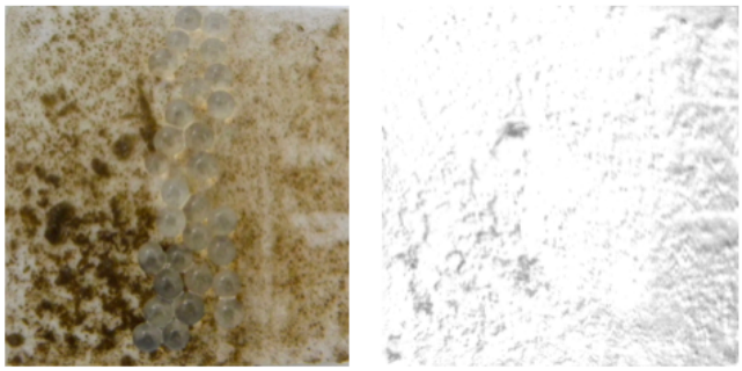

Figure 5.6: **Selective growth induction using alginate capsules.** The capsules containing 0,1% w/v glucose were placed on a biofilm growing on ceramic tale (A). B - optical image subtraction at day 6. Grey: indication of increased biomass, white: no change.

A matured biofilm was partially scrubbed from ceramic tile using kitchen paper. Alginate capsules, prepared as mentioned above, were impregnated with 0.1% w/v glucose. The capsules were placed in a line in the center of the ceramic tile (Figure 5.6 A). During the first two days the water, with the submerged ceramic tile, was supplied with sodium iso-citrate (0.1 M) solution. Figure 5.6 B shows the difference of biomass between day 0 and day 6. The results suggest that biomass mainly developed around the capsules (grey: biomass accumulation, white: no change). While the capsules themselves hinder biofilm formation, they can be used as tool to enhance biofilm growth in regions proximal to their location.. D3.3.5 Validation of the delivery of compounds of interest using OCT imaging A similar experiment was conducted to prove the biofilm accumulation with help of OCT. A biofilm grown on a ceramic tile was scrubbed completely using kitchen paper. The ceramic tile was then placed in tap water. Alginate capsules (3% w/v sodium alginate in tap water and 0.1% w/v glucose) were added to the top part of the ceramic tile as shown in the followijg image.

For two days, 10 ml of sodium citrate (0.1M) was added daily to the tap water. The beads were removed after 5 days and replaced by new capsules containing higher glucose concentration (1% w/v). Sodium iso-citrate injections were then performed on day 6 and 7. The OCT images were captured between each change of the conditions (day 0, day 5, day 19), see

The results of 3D OCT image analysis indicate that controlled delivery of small compounds of interest (glucose) to the biofilm is possible using alginate. This validates the findings from before. The alginate beads, containing the only carbon source for the bacteria, can be used for selective growth of biofilm adjacent to their position.

Figure 5.7: **Scheme of capsules positioning on the biofilm surface.**

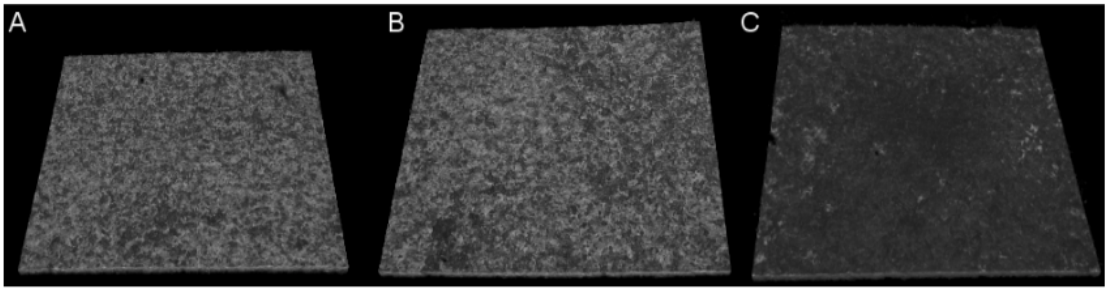

Figure 5.8: **3D OCT images in the center of the tile at day 0 (A), day 5 (B) and day 19 (C).** Biofilm formation is clearly visible towards day 19. Imaging area was 5 mm x 5 mm.

5.2.4 Introducing the alginate capsules carrying nutrients into the MFCs

To ensure the stable power output of the anodic biofilm and to investigate the potential delivery mechanisms for the compounds of interest, alginate capsules were introduced with the help of KIT collaborators into the MFCs operating in fed-batch mode while the open circuit voltage was monitored continuously. To prepare the capsules containing the compounds of interest, sodium alginate was dissolved into concentrated (100 x) nutrient solution and used to produce 4 types of alginate capsules: capsules containing only nutrient solution, capsules supplied with 1% w/v glucose, acetate or iron sulfate. Once prepared, the capsules were washed with deionized water, dehydrated and introduced to the MFCs. Glucose, acetate and nutrient capsules were introduced in the anodic chamber and iron sulfate capsules into the cathodic chamber. Iron enriched capsules, as redox- mediator for electron uptake from the cathode, were introduced to MFC1 one week before introducing the capsules carrying nutrients and carbon sources. For the MFC2 the iron capsules were introduced simultaneously with the nutrient-containing capsules. The final experimental setup was as follows: MFC1: glucose capsules anode, iron sulfate cathode; MFC2: acetate capsules anode, iron sulfate cathode; MFC3: nutrients capsules anode.

Introducing the capsules containing glucose as a carbon source resulted in an increase of the OCV. The effect of the capsules started two days after they were introduced into the system. Two days of adaptation period, which is relatively long for such an easily accessible substrate, suggests that glucose was slowly released into the feedstock. Nevertheless, the lag-phase observed for acetate suggests that the complete

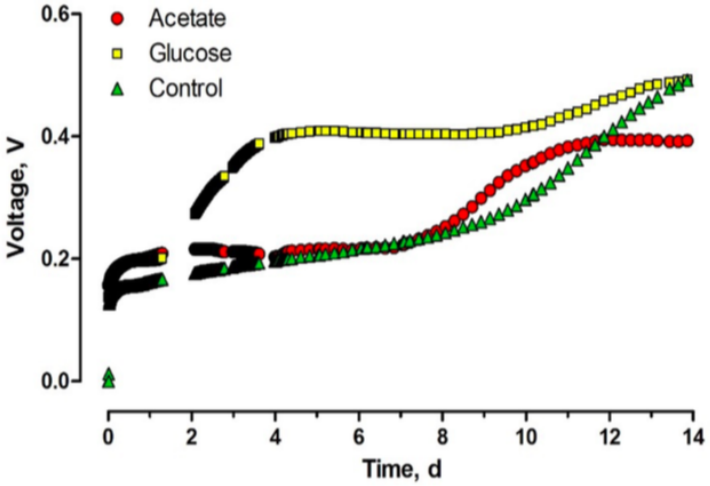

Figure 5.9: **Open Circuit Voltage (OCV) of Microbial Fuel Cells supplied with the capsules carrying the substrates: glucose (MFC1), acetate (MFC2) and nutrients containing control (MFC3).**

release of this substrate from alginate capsules took place before the bacterial cells started to utilize the first portions of nutrient diffused from the capsules.

5.2.5 Integration of the robotic, chemical and biological platforms

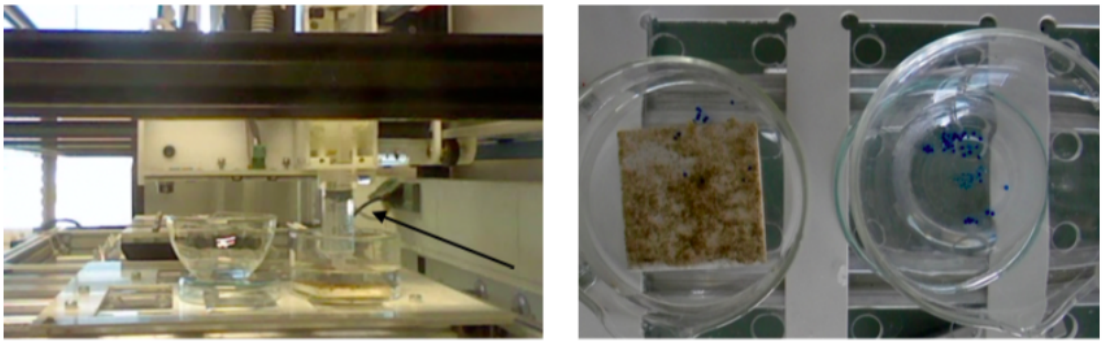

Figure 5.10: **Robot adding the alginate capsules from the stock vessel to the biofilm experiment (the arrow indicates the syringe).** A) Overall setup with the arrow indicating the position of the syringe and B) top view onto capsules dispensed on biofilm grown on a ceramic tile.

The Evobot platform was used to either remove or distribute the dehydrated alginate capsules over the biofilm surface and outside the growth area (as control), see Figure 5.10 and movie D.3.3.3 (`https://youtu.be/9mShxqo7D4U`). The same principle can be adapted to introduce the capsules into the anode or cathode chambers of the MFCs.

5.2.6 Tests with magnetic nanoparticles

To explore the potential of repositioning the nutrient-carrying alginate capsules in non- invasive manner, the alginate capsules were impregnated with the magnetic nanoparticles. The alginate was dissolved in tap

water (3% w/v) and two types of capsules were prepared, containing: 7 ml of alginate and 30 μl Pelikan blue ink (light blue capsules) or 70 μl of blue ink and the magnetic nanoparticles (brown capsules). After polymerization capsules were dehydrated and placed in a petri dish (8 cm diameter) filled with tap water. As shown in Movie D3.3.4 (https://youtu.be/LrWk3poZnJ8), by applying the magnetic fields it is possible to reposition the impregnated capsules containing magnetic nanoparticles (also see Figure 5.11). As expected, the control sample (light blue capsules) does not show any movement induced by the magnet.

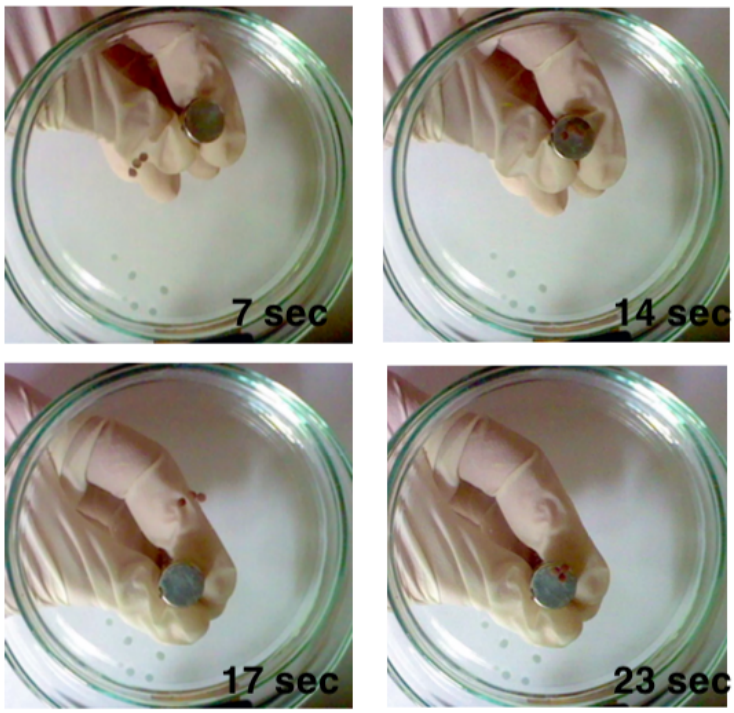

Figure 5.11: **Using the magnetic field for spatial redistribution of the alginate beads containing magnetic nanoparticles.**

The results indicate that the Evobot (modified with a magnet) can be employed for spatial and temporal redistribution of the capsules. This will allow to selectively distribute nutrients or magnetic nanoparticles onto the biofilm. Furthermore, more complex compounds, such as biocatalyst, could be used to improve the performance of MFCs or help to stabilize the power output. Introducing the magnetic nanoparticles may minimize the mechanical impact of the rigid elements of the robotic platform on the biofilm structure, if needed.

5.3 Discussion

We have demonstrated several approaches that integrate the chemical artificial life with living biofilms using the robot. The chemical droplets can still function chemotactically in the presence of the living biofilm, but they are largely bio-incompatible (e.g. chloroform) and result in the reduction of the biofilm growth and reduction of the output from the MFCs. Knowing that decanoate chemotaxis works even at pH 7 and with other surfactants maybe more biocompatible (see chapter 6) a future prospective could be for sure to test this new chemotactic system in presence of biofilms and MFCs.The alginate system was useful for demonstrating the controlled introduction of impregnated alginate to the living biofilm using the robot. The biofilm growth was enhanced when the alginate was impregnated with a carbon source such as glucose. In addition, the output from the MFCs was improved. For future robotic control over both the chemical and biological system, magnetic nanoparticles may prove to be a control mechanism of choice. In the end we were able to demonstrate that the chemical systems (decanoate pH 12) was detrimental to the growth, structure and output of the living systems. Instead the alginate system showed positive effects on both the growth of the living biofilms and the output of the MFCs. We used the robotic platform to demonstrate the controlled spatial and temporal deposition of alginate capsules on living biofilm.

5.4 Material and Methods

Materials

All reagents for the chemotaxis experiments were supplied by Sigma Aldrich: decanoic acid, 1-decanol, Oil red O, sodium hydroxide, sodium chloride, sodium alginate, chloroform, sodium isocitrate, glucose, acetate and iron sulfate. Blue ink was obtained from pelikan.

Methods

Unless otherwise specified, experiments were carried out at room temperature.

5.4.1 Biofilm and droplet interaction

Biofilm cultivation was performed on ceramic tiles of size 4 cm x 4 cm for approximately 30 days using a fume with low COD concentrations. The petri dish was filled with 20 ml of decanoate 5 mM pH 11, the droplet (20 μl and coloured with Oil red O empirically until that the desired color was obtained) placed upon it and moved using 3 M NaCl. Biofilm was afterwards imaged with OCT.

5.4.2 Alginate and biofilms

Alginate capsules were prepared by dissolving sodium alginate (3$\%$ w/v) in tap water. Two types of capsules were prepared, containing different concentrations of glucose (0,1$\%$ and 1$\%$ w/v). The capsules were extruded using a 20 ml syringe with a 0,8 mm gauge needle into a calcium chloride (CaCl2) 1$\%$ w/v solution. The capsules were cross-linked for 1 minute and then CaCl2 solution was poured away. The capsules were dehydrated for two hours at 100° C. After dehydration the capsules were placed on the surface of biofilm. Biofilms were then covered with a layer of tap water. For the first five days of the experiment, each sample was supplied with 10 ml of 0.1 M sodium citrate solution at 1-day intervals as

a potential nutrient but also to chelate the calcium ions and slowly dissolve the alginate capsules. On the sixth day, tap water and the residuals of dissolved capsules were removed and optical images of the biofilms were taken using a Nikon camera. The images were then processed, using Fiji software.

5.4.3 Introducing the alginate capsules carrying nutrients into the MFCs

Alginate capsules were introduced with the help of KIT collaborators into the MFCs operating in fed-batch mode while the open circuit voltage was monitored continuously. Sodium alginate was dissolved into concentrated nutrient solution and used to produce 4 types of alginate capsules: capsules containing only nutrient solution (100 x compared with normal nutrients with which MFCs were fed), capsules supplied with 1% w/v glucose, acetate or iron sulfate. Once prepared, the capsules were washed, dehydrated and introduced to the MFCs. Glucose, acetate and nutrient capsules were introduced in the anodic chamber and iron sulfate capsules into the cathodic chamber. Iron enriched capsules, as redox- mediator for electron uptake were introduced in the cathodic chamber.

5.4.4 Tests with magnetic nanoparticles

Alginate was dissolved in tap water (3% w/v) and two types of capsules were prepared, containing: 7 ml of alginate and 30 μl Pelikan blue ink (light blue capsules) or 70 μl of blue ink and the magnetic nanoparticles (brown capsules). Capsules were cross-linked, dehydrated and placed in a petri dish (8 cm diameter) filled with tap water (10 ml).

We used our collaboration with ITU of Copenhagen to expand the types of aqueous phases that could be used in our droplet chemotaxis experiments using their robotic workstation as part od the Horizon 2020 EVOBLISS project. We explored new surfactant phase, modified the algorithms and tracking in way to develop the efficiency and the velocity of droplet chemotactic movement under new conditions, as detailed in the next chapter.

Chapter 6

Characterization of droplet movement, tracking and evolution

An important part of the work performed during this years was to test, characterize and try to evolve the 1-decanol droplet system. I've tested not only chemotaxis protocell systems, but even, as cited before, shape change and rudimentary fission-fusion cycles as shared with us from our collaborators in Glasgow [67]. An example of reproduced system that shows fission is a droplet of 1-octanol and Diethyl phthalate (DEP) mixed 1:1 in 20 mM aqueous tetradecyl- trimethylammonium bromide (TTAB). The droplet when placed in the water phase instantaneously divides into many smaller ones (see `https://youtu.be/aGPhh8pPK7I`). There are additional cases instead when the fission appears like a droplet dividing into two and afterwards droplets connect each other and interact through their interface. This behaviour is shown for example with 1-octanol and DEP mixed with a 20-80 % ratio (see `https://youtu.be/WKI9jdIiOdQ`). In the case of 1-octanol-DEP mix, fission can be explained as a reduction of the energy of the system. This could be interpreted as an high pH interaction of positively charged TTAB and 1-octanol that interact due to their opposite charge exposing DEP from droplets surface. DEP when exposed becomes negatively charged and induces even through its hinderance droplet fission.

6.1 Results

6.1.1 Characterization of 1-decanol chemotaxis

With the help of Carlotta Porcelli we well characterized the chemotactic behaviour of 1-decanol droplet in decanoate (high pH) after the addition of usually 3 M NaCl solution. Figure 6.1 shows the droplet lateral displacement recorded in 8 experiments, the setting is shown in Figure 1.1 and following described.

For velocity analysis of droplet movement during chemotaxis, eight experiments were performed under standard conditions: 9 ml of decanoate 5 mM pH 11, 450 μl of sodium chloride 3 M, 20 μl of 1 decanol colored with 0.2 mg/ml Oil Red O. The tracking of the droplet position lasts for one minute and begins when the 1-decanol droplet starts to move from its initial position. The initial position is defined by a circle with a specific diameter of $3\times$ the droplet diameter surrounding the point where the droplet is initially placed. This is necessary to avoid measuring initial fluctuations in droplet position that are common before the chemotactic movement begins. The tracking algorithm calculates the droplet velocity for each time frame and the mean of the calculated values was used to obtain the droplet mean velocity.

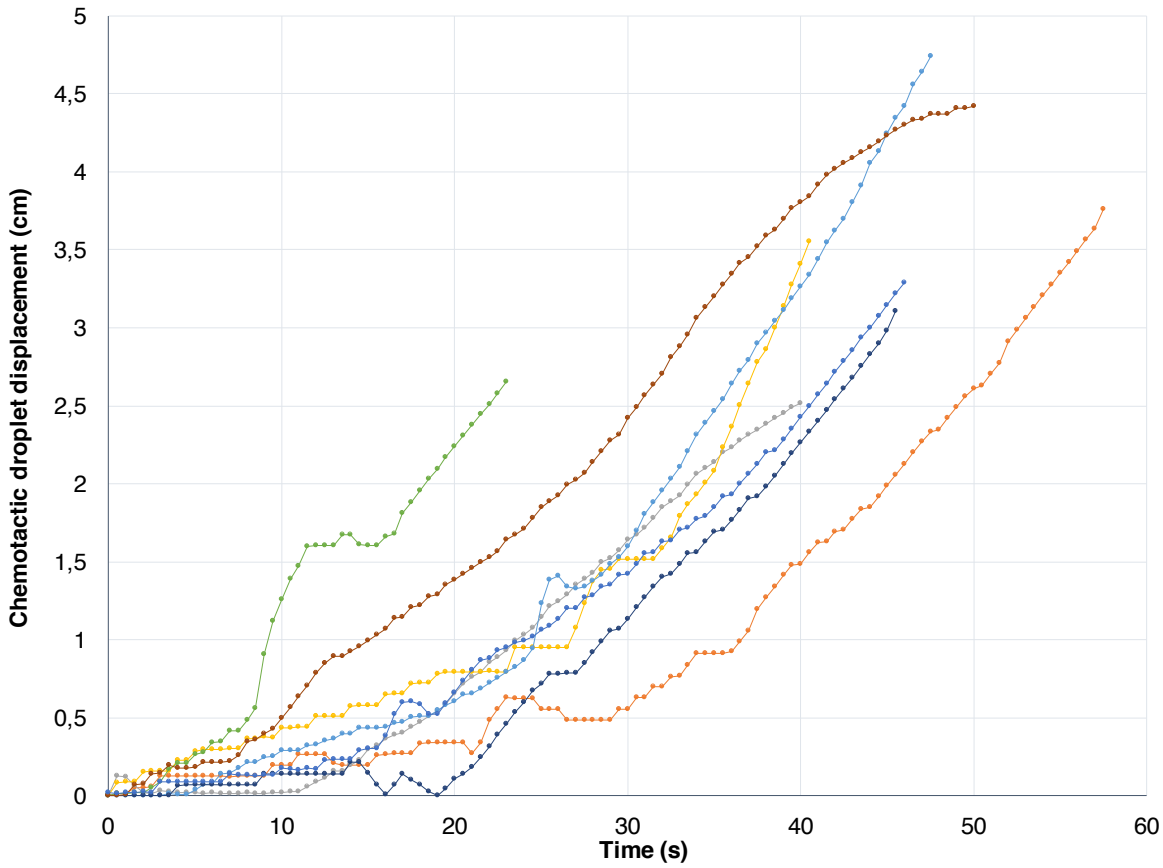

Figure 6.1: **General tracking of droplet-mediated transport experiment.** Eight experiments of 1-decanol droplet chemotaxis inside decanoate solution (5 mM pH 11, 200 μl of 3 M NaCl) were performed. Videos were analyzed (see methods 3.2.1 for more details) for the time resolved displacement (y-axis) over time. Each point represents a 0.5 second interval. Each droplet is represented by a different colored line.

The standard deviation was obtained from the 8 experimental replicates. The mean velocity of droplets after the addition of 450 μl of 3 M NaCl is 0,049 $\pm$ 0,007 cm/sec.

The eight experiments were tracked using EVOBOT (see `https://real.itu.dk/people/afaina/attachment/20/`) and the results were analyzed using a free software: 'Tracker - Video Analysis and Model Tool' (see `https://physlets.org/tracker/`). The video analysis has been performed setting a reference measure from the 'real object', in this case the 9.00cm of the Petri dish diameter. The changes of position of the droplet are registered in each frame. Data are shown in Figure 6.1, where droplet displacement from the origin to the point of salt addition are plot against time.

6.1.2 EVOBLISS project

Our collaborators at ITU were our partners in EVOBLISS project (`https://blogit.itu.dk/evoblissproject/`). "The EVOBLISS project is part of the cluster of projects funded by the E.C.'s Future and Emergent technologies proactive on evolving living technologies (EVLIT). The challenges addressed by this call is to explore the potential of the computational and self-adapting properties of living organisms for future ICT technology because these properties of living organisms are superior to what can be found in today's ICT technology.' The aim of EVOBLISS project is to develop artificial, technological evolution and use it to design functional ecosystems consisting of up to three forms of living technology, namely, artificial chemical life, living microorganisms, and complex chemical reaction networks for the purpose of improved treatment and cleanup of wastewater for energy generation. The goals of this project are i) develop a general, robotic platform, which by using artificial evolution can optimize the performance of a physicochemical or microbial system and its environment and ii) use the robotic platform to evolve improved microbial fuel cells in terms of robustness, longevity, or adaptability. The name of the robotic platform is EVOBOT. The robot evolutionary platform will take the form of an open-source 3D printer extended with functionality for handling liquids and reaction vessels, and for obtaining feedback from the reaction vessels either using computer vision or task-specific sensors in real-time. The robot platform will optimize parameters such as the environment, hydraulics or real-time interaction with experiments (for instance, timing of injection of nutrients, removal of metabolic products, stirring, etc.) to maximize a desired functionality. Initially, we investigate processes such as fluid-structure-interaction driving bio-aggregate structure and in turn metabolic activity as well as the interaction of nanoparticles and bacterial cells by analyzing the outcome of the evolutionary process using state-of-the-art imaging techniques. We then seek to exploit synergies between these technologies to significantly improve the ability of the living technology, in the form of optimized microbial fuel cells, to cleanup wastewater. Overall, this is a cross-disciplinary project involving state-of-the-art chemistry, imaging, robotics, artificial life, microbiology and bio-energy harvesting for the purpose of enhancing our understanding of living technologies and how to best design and exploit groundbreaking bio-hybrid systems." [68]

6.1.3 Chemotaxis optimization

As said before, the goal of this project is to develop EVOBOT, a general, robotic platform, which by using artificial evolution can optimize the performance of a physicochemical system such as the chemotaxic one. Evolution can for example be defined as a process during while system variation produce benefits that create a selection and a population drift over generations. Variations that give benefits are in this way passed through generations to produce individuals with increased benefits. The evolution we will deal with is artificial and the benefits we would like to achieve are a faster, more precise and in more physiologically compatible environment chemotaxis. This evolution can be more precisely defined as a system optimization. It is an evolution, but the number of compounds used in our experiments is low, there are no chemical reactions happening and mutations that could happen but simple what could be defined as changes of state, there is no genetic material present in our system that mutating could show a variation in phenotype and the number of generation we run is not comparable to an evolutionary significant one.

EVOBOT is composed by different layers, an experimental layer where petri dishes and beakers with surfactant solutions are placed, an upper layer, composed by the head, in which dispensing syringes are located and a bottom one where a video camera to record the tracking is placed. All the experiments are

dispensed, recorded and analyzed using python coding and computer interface. We hypothesized and tested different fitness functions to describe the chemotactic displacement during our experiments and tried to optimize it towards desired outcomes such an increase in velocity or efficiency in salt reaching and conditions more conducive to physiological ones (pH 7). Our experiments were sometimes noisy and after many trials we were able to create a fitness function able to describe 1-decanol displacement (Figure 6.2) and to be implemented and used by EVOBOT. The initial position of the droplet is set as when the tracking starts is indicated by the circle 0. The starting position of the droplet is recognized by the software and a small safety area with a fixed radius is drew around it. Droplet is tracked when leaves this safety area. A fitness value of 0.0 is assigned to the individuals which do not leave the safety area. On the other hand, when the droplet leaves the safety area, the distance between two positions 8 frames away from each other is computed. The directional vector of the droplet path is projected on the direction between the droplet's starting point and the salt addition point, see Figure 6.2, and the partial fitness is computed. The tracking stops after 80 seconds. The final fitness value is obtained dividing the sum of all the relative fitness values by the total number of frames of the video registered. The formula used to calculate the fitness function is following reported and visually described (f(x) stands for the projection of the droplet path on the vector between the droplet's starting point and the salt addition point).

$$F = \frac{\Sigma\, f(x)}{x}$$

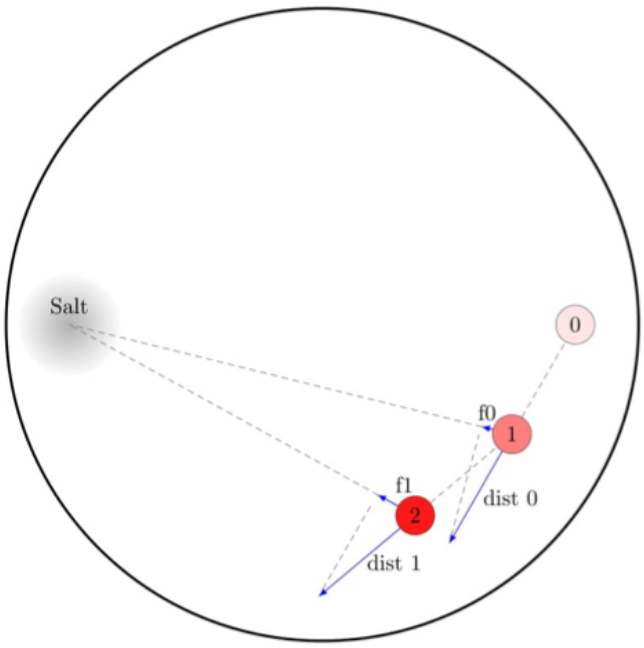

Figure 6.2: **Fitness calculation.** The initial position of the droplet when the tracking starts is indicated by droplet 0. After eight camera frames (x), the droplet has moved to position 1. The vector dist 0 is projected on the axis droplet-salt and the partial fitness, f1, is calculated. The same procedure is repeated every eight frames. The total fitness is the sum of the partial fitness divided by the number of frames.

Our chemotaxis experiments are normally performed at high pH (11-12), to render the experimental

conditions more conducive to physiological ones, we tested at UniTN the droplet chemotaxis in decanoate 5 mM pH 7. This less harsh condition efficiently produced chemotaxis and we decided to spam chemotaxis in different decanoate solutions with pH going from 7 to 12.3 and varying molarities. We decided to set the experiments in the following way: the experiments are based on two phases, one is fixed and the other one is variable. Oil and salt are fixed phases, molarity (between 5 and 20 mM) and pH (7-12.3) of the decanoate water phase are instead varied in each experiment. We run 8 experiments each generation and The Covariance Matrix Adaptation Evolution Strategy (CMA-ES) was chosen as the evolutionary algorithm. This algorithm produces good results even with a low number of evaluations, in this case we run 8 experiments in each generation. Real numbers from 0 to 1 represent the two variables of the experiments (pH and molarity). The algorithm uses the generate-update paradigm where a population is generated from a strategy and the strategy is updated from the population. Each generation is composed of 8 individuals and the starting point of the first generation is the centre of the search space (0.5, 0.5). This point represents pH 9.65 and molarity 12.5mM, the initial step-size () is 0.15. CMA-ES belong to the class of evolutionary algorithms. In each generation (iteration) new individuals are generated by variation, usually in a stochastic way, from the current parental individuals (the parental individual of the first generation is [0.5, 0.5]) and the following individuals are generated using a variation of 0.15. Then, the individuals resulting with the best fitness value are selected to become the parents of the next generation. This process runs for 10 generations where individuals with increasing f-values are selected in each iteration. In the case our optimization would be successful we expect to have an increase in the mean fitness value and a condensation of f-value dots in a small area, after an initial spread following the first generation (in our case generation 1).

We run in collaboration with ITU 15 generations. The results are reported in Figure 6.3 and 6.4.

The fitness values obtained from this 'optimization' clustered, during generations, inside a region with reduced molarity and pH but did not show any specific trend in the mean value fitness of each generation. This is due to the fact that experiments were still noisy and with a lot of random movements. For sure we would need to run more generations and with an increased number of individuals but we decided to start modifying some experimental settings and some fitness function specifications.

We tried to limit the amount of spurious 1-decanol droplet movements. We tested whether we could limit the noise of the system trying to reduce: 1) the evaporation of 1-decanol into the air space and 2) the dissolution of 1-decanol into the water phase. To do this we tried to isolate bodily each chemotaxis experiments. ITU built a lid module to move a lid up and down and to rotate it. The lid does not only reduce the air movements but even gives a white background to the experiment and facilitates the tracking that is based on color recognition. This avoids moving the head from the field of vision of the camera after the liquid pull. We also limited 1-decanol dissolution by first saturating the aqueous phases with 1-decanol. This idea according to previous experiments performed in Trento, in which I was able to run efficiently chemotaxis even in saturated decanoate at pH 7. According to the results obtained with ITU the presaturation of the aqueous phase with 1-decanol reduces noise and produces more reproducible results. The effect of the lid is also noticeable and produces higher fitness scores (see Figure 6.5, orange points for experiments covered and using saturated decanoate).

However, as said before, the graph of the fitness of the best individual and the average of the population shows that neither of them improves over generations (see Figure 6.4). So we decided to modify even fitness and our tracking program. The tracking was stopped as soon the droplet reaches the edge of the

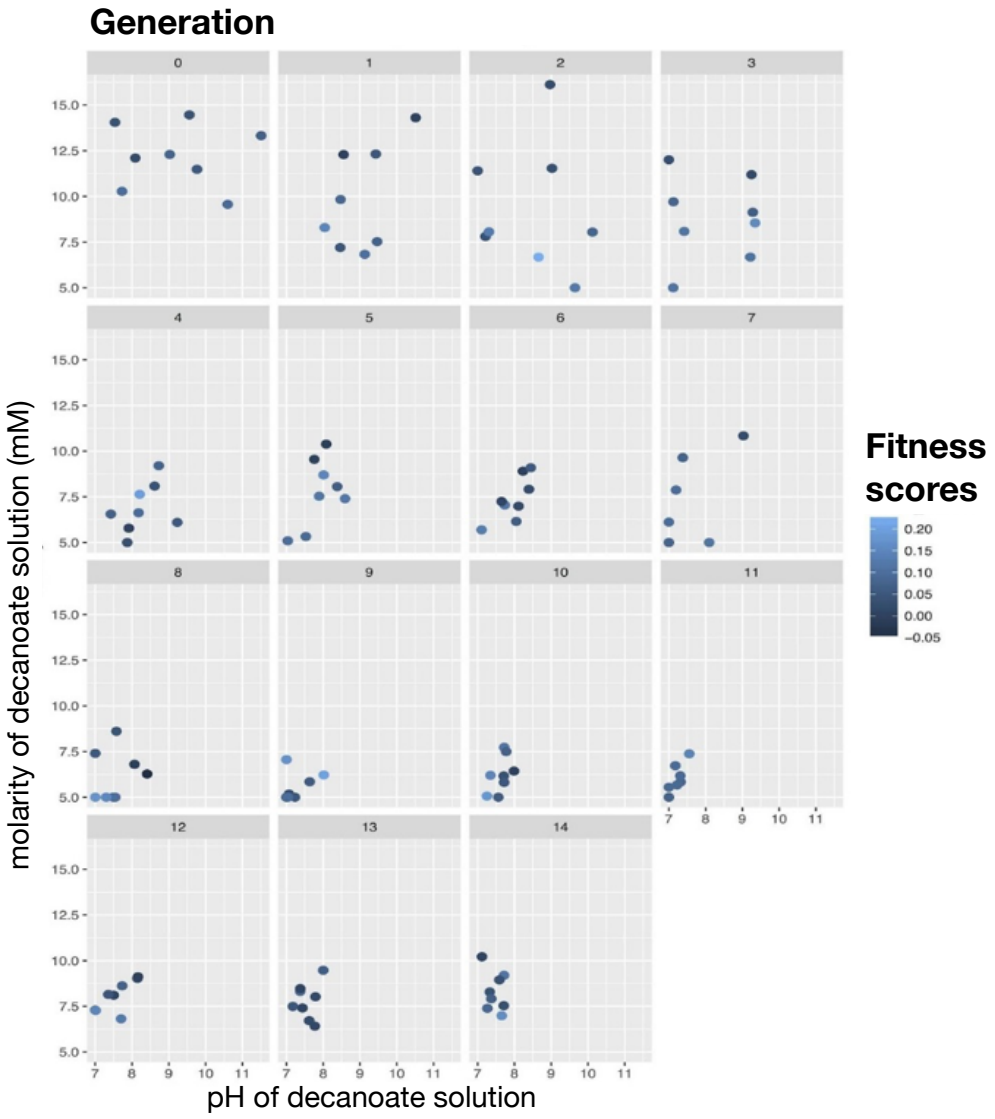

Figure 6.3: **Fitness over 15 generations.**

Petri dish or as soon as the direction of the droplet was too different from the salt direction. The final fitness is obtain as the sum of the partial fitness divided by a constant (100) and the number of frames. This constant penalises short movements towards the salt that are stopped after a few frames. We obtained in the following generations a new kind of trend, with a slight increase in the median fitness (see Figure 6.6).

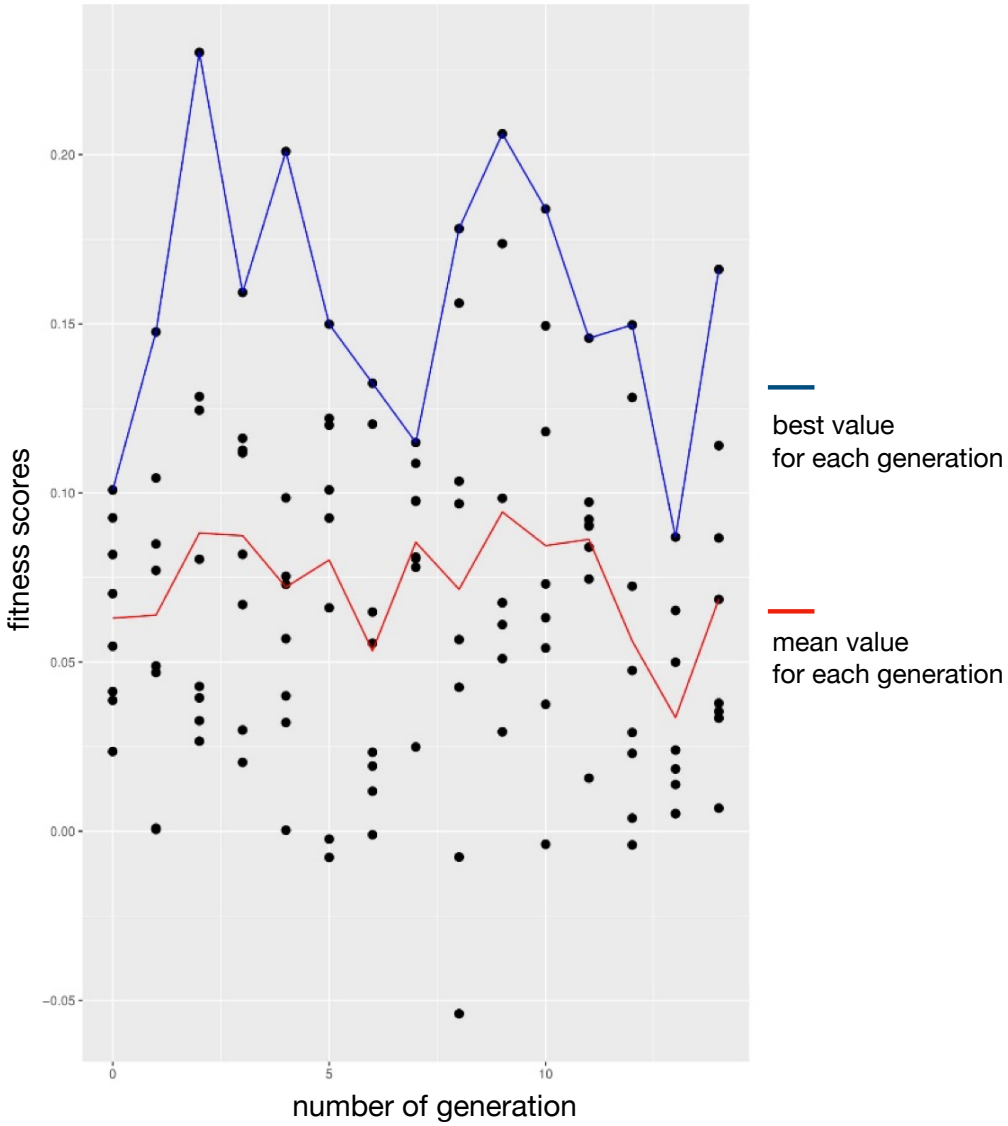

Figure 6.4: **Mean fitness over 15 generations.**

6.1.4 Optimization of the chemotactic system using new surfactants

At this point we used this last developed new fitness function to test new experiments with enlarged research space. Before doing this I tried to enlarge the reseach space manually, testing new chemicals one by one. The enlarged space chosen for the oil phase was: 1-hexanol, 1-heptanol, 1-nonanol, 1-undecanol, hexane, heptane, octane, noanane and undecane. The enlarged space chosen for the water phase was: SDS (anionic surfactant), CTAB (cationic surfactant), polyethylene glycol (PEG), Tween 20 and Triton X 100 (bith three as non ionic surfactants). I manually performed experimental triplicates of decanol chemoatxis in all the possible composition of the water phase (pure or mixed 1:1). Knowing that chemotaxis in decanoate works at a concentration that is 1/10 of decanoate critical micelle concentration (cmc) we tested all the other surfactants dissolving them in water at 1/10 cmc. I could see an outcoming behaviour in the following cases: 1-decanol in PEG (slow chemotaxis after a starting random movement), 1-decanol in Tween 20 (division and when the droplet is stabilized a slow chemotaxis during which the droplet still tries to split), 1-decanol in PEG and decanoate mixed 1:1 (chemokinesis) and 1-decanol in decanoate and

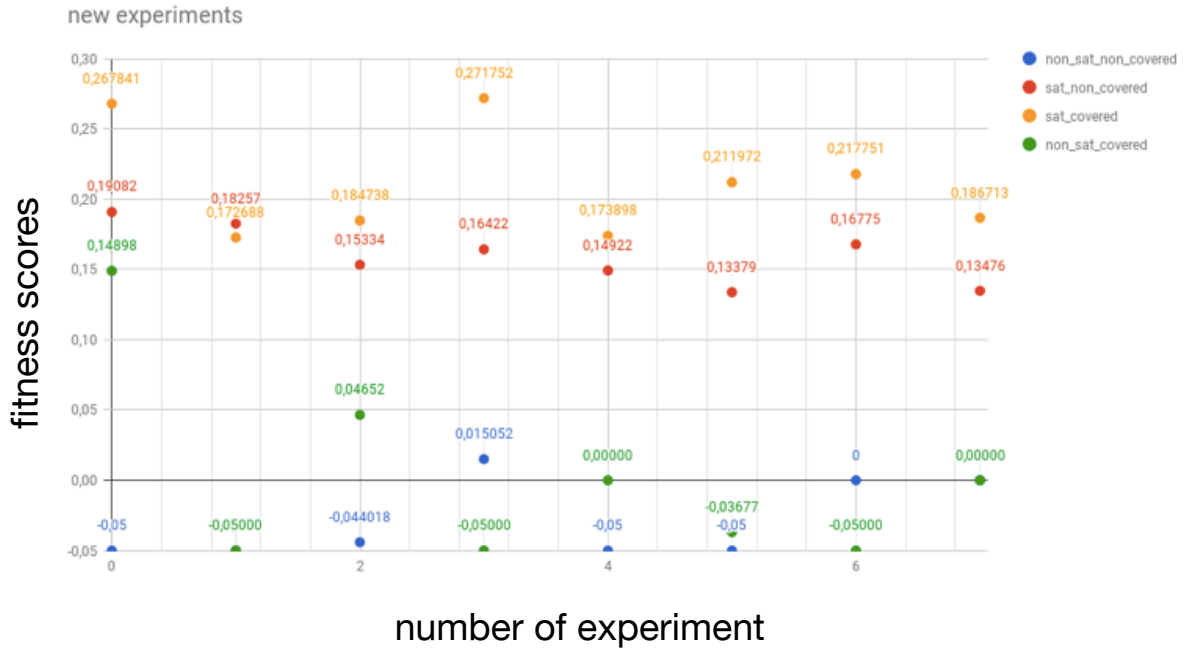

Figure 6.5: **Fitness evolution.** Fitness obtained for seven experiments with four different experimental settings with pH 7 and molarity 5 (blue for no saturation and no coverage, red for no coverage and saturation, green for coverage and no saturation and orange for coverage and saturation). The effect of the saturated solution and the lid produces higher fitness scores (orange points).

Triton X 100 (opposite chemotaxis). This experiments were preliminary research for the droplet evolution performed with ITU.

At this point we tried to enlarge the chemotaxis research space used from the robot and tested the new chemotactic chemical water phases: PEG and TritonX100. We evaluated the chemotaxis experiments, scored them empirically and using EVOBOT. We obtained a similar trend of the values obtained with the fitness functions to the ones that we empirically scored in the experiments in Trento. We have used EvoBot and CMAES to evolve the conditions for the oil droplet chemotaxis experiment towards more physiological conditions. Further improvement in the design of the experiment by reducing the noise should allow for more efficient optimization of the experimental conditions and to enlarge all the research spaces, even for example the oil and salts tested.

6.2 Discussion

With the help of our collaborators at ITU we improved the settings of EVOBOT robotic platform and optimized algorithms used for the chemotaxis experiment. We started four years ago with only one experiment examined on the experimental layer and a rudimental tracking (comparing the distance between salt addition point and the droplet end up point with the distance between the end up and starting point of droplet). Now we have 8 experiments each generation and a tracking able to show fitness values convergence and slight mean fitness optimization. We had sometimes noisy outcomes but we were able to demonstrate that EVOBOT can be efficiently used to dispense the liquid phases required in our experiments, to track our droplet movement and to 'evolve' the chemotaxis towards conditions more

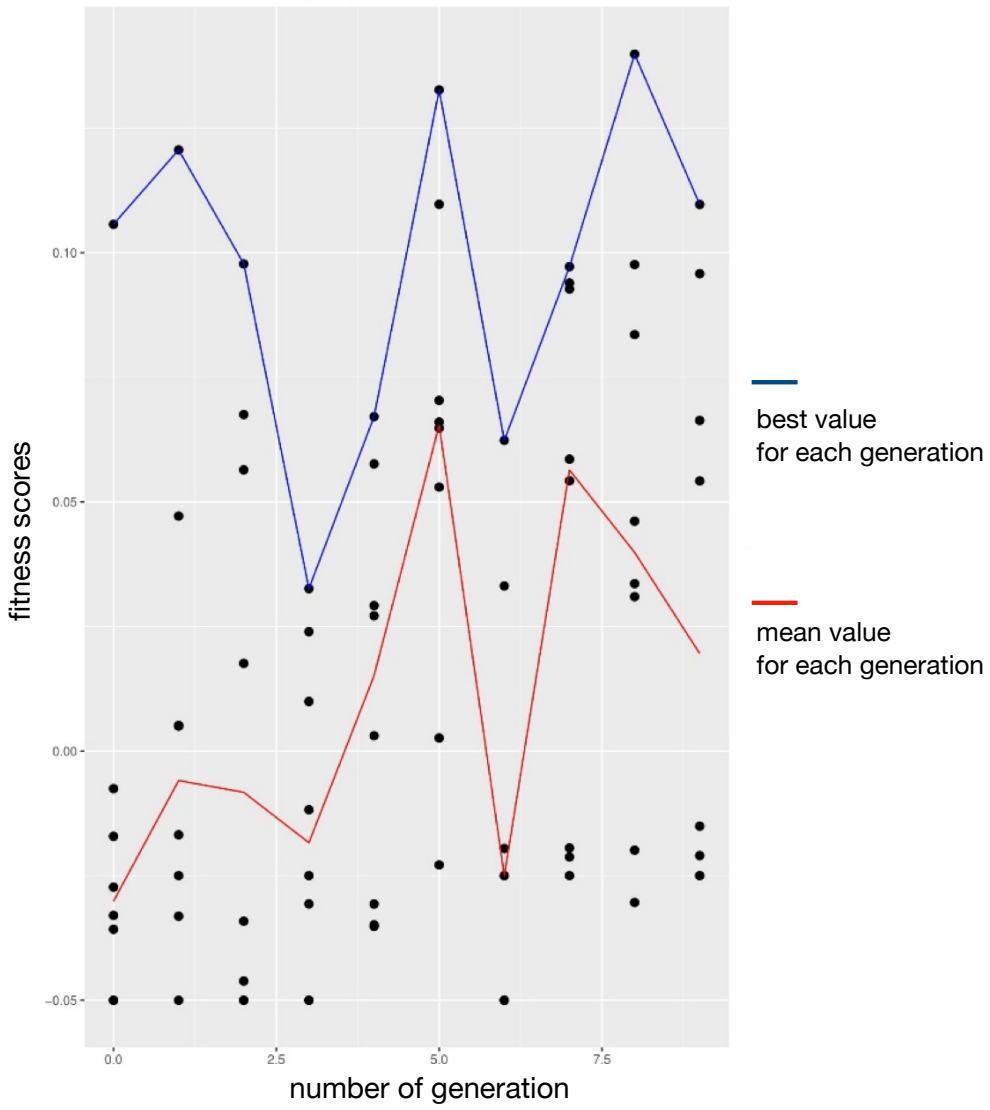

Figure 6.6: **Mean fitness over 10 generations.**

conducive to physiological ones. We had no 'real' evolution but an optimization of the efficiency and of the chemotaxis conditions. Over 15 generation we showed no evolutionary significant increase of fitness function and a slight convergence towards values and a compression to a region with decreased pH and molarity (see Figure 6.3 and 6.4). However varying few parameters we obtained a slight increase in the overall generation fitness (see figure 6.6). We showed this kind of tracking is applicable to an increased research space with new compounds. Probably this kind of chemotaxis experiments are not the best suited, due to their intrinsic noise, to show a significant over generation evolution but simply an efficiency optimization. Both two experimental settings and fitness function can still be implemented, however EVOBOT could be a well suited 3D standalone platform to run this kind of experiments.

6.3 Material and Methods

Material

All reagents for the chemotaxis experiments were supplied by Sigma Aldrich: decanoic acid, 1-decanol, Oil red O, sodium hydroxide, sodium chloride, calcium chloride, PEG, Triton X 100. Glass DURAN Petri dishes were supplied by Fisher, syringes from PIC and Glass slides from Prestige.

Methods

Experiments were carried out at room temperature.

6.3.1 1-decanol chemotaxis

All the experiments were performed using EVOBOT: the experimental layer was filled with petri dishes, the syringes on the head loaded with 1-decanol or 3 M NaCl, the beakers on the experimental layers filled with water phases highly concentrated in surfactants and the water pump prepared. Glass Petri dishes of 9 cm diameter were filled with a total volume of 9 ml surfactant solutions: starting from decanoate, PEG and Triton X 100 solutions highly concentrated and diluted using *milliQ*water. Droplets of (10 μl) 1-Decanol (colored with Oil red O) were added from EVOBOT to the system and moved using 3 M NaCl. Droplet chemotaxis movement was tracked using EVOBOT.

Chapter 7

Future perspectives

I was able during these four years to create a stable system able to transport alginate capsules.

An interesting future perspective could be to move alginate droplets enriched with chemicals, able to be released from their capsules, and maybe react with free enzymes or within a specific type of cell. Small bioactive compounds can be encapsulated and released from capsules as shown by Kikuchi et al. This group studied the dextran release from alginate capsules. They focused on release of dextran with different molecular weights from alginate capsule calcium crosslinked [69] and its pulsed release through the use of capsules of different sizes [70]. There were many studies on active compounds release, in 2018 of Nikoo et al. studied the diffusion of caffeine from alginate hydrogels and related its release to Fick's diffusion law. It could be feasible to create a transport and drop system of capsules enriched with specific compounds able to start specific reactions with elements present in the targeted position of our transport. Otherwise, knowing that we can transport more capsules together increasing the droplet volume or move more than a droplet each time, we could imagine coupling the chemotaxis of one droplet carrying cells with another one carrying a specific bioactive compounds.

The experiment that could work most reliably would be the transport of an eukaryotic cell line able to proliferate in DMEM, not sensitive to 1-decanol and encapsulated in alginate dissolved in water phase from A549 cells mixed 1:1 with water. We could try to use other types of chemotaxis system to transport the capsules, such as the one tested in the evolutionary experiments with KIT: PEG, triton etc. Few of these systems could have less detrimental conditions for eukaryotic cells survival. Knowing the toxicity of 1-decanol repeating the droplet evolution introducing new and less poisonous oil phases could give us a lot of new exploitable possibilities.

The alginate capsules could be further refined as well. We can for example create an outer shell for the capsule by incubating the capsule a second time inside the alginate gel and dropping the gel surrounded capsule in the calcium chloride solution. This shell can be produced with alginate dissolved in different water phases going from decanoate to A549 water phase and could protect the cells form 1-decanol and from decanoate pH 12 used for the capsule release. Even the alginate stiffness (w/v $\%$ of alginate dissolved in water) of the inner capsule could be varied. Being only the external shell in contact with 1-decanol the internal w/v alginate percentage could be in fact reduced this enabling the survival of cell lines even more sensitive to growth conditions than A549 cells. It is however difficult to control the dimensions of the capsules with shells and a drying step before the transport would be needed to reduce the capsule weight and allow their transport. Otherwise we could use different techniques for the creation of smaller and

more homogenous capsules. Many techniques exist for the creation of micro-molded alginate capsules. Micro alginate gel beads were first created by Ogbonna et al. in 1989 using a rotating disk atomizer with variable rotation speed and varying the flow rate of alginate solution [72]. Nowadays, photolithography and micro- and nano-imprint lithography are promising new options for the creation of drug delivery micro carriers. Micro-molding processes are well-developed and can easily be adjusted to create well-defined two-dimensional and three- dimensional structures of varying shapes and sizes [73]. However, creating an external shell already compatible with decanol from its creation, the DMEM incubation would not be needed anymore and other types of cells could be transported and survive efficiently.

Chapter 8

Aknoledgements

I would like to thank Martin Hanczyc for having been my mentor and tutor during these 4 years, for his incredible support, for the research ideas that always gave great results, for letting me be part of EVOBLISS (all the meetings and all the presentations that gave an incredible improvement in my scientific preparation) and for having tolerated all the times that I have arrived to the lab with a bone or muscle broken.

I would like to thank too all the lab mates and friends that I knew in all these 4 years and to remember all the CIBIO happy hours we had together.

And thank you Carlotta Porcelli for all the times you corrected my latex compilation errors.

Bibliography

[1] ALIFE 2018, the conference on artificial life 2018, tokyo 23-27 july 2018

[2] Leduc, S., The Mechanism of Life. William Heinemann London, UK: 1914

[3] Hanczyc, M.M.; Fujikawa, S.M. and Szostak J.W., Experimental Models of Primitive Cellular Compartments: Encapsulation, Growth, and Division, Science 302(5645), 618-622 (2003)

[4] Tsuji, G., Fujii, S., Sunami, T., and Yomo, T., Sustainable proliferation of liposomes compatible with inner RNA replication. PNA, 113(3) 590-595 (2016)

[5] Chen, I.A. and Waldez, P., From Self-Assembled Vesicles to Protocells. Cold Spring Harb Perspect Biol (2010)

[6] Li, M., Huang, X., Tang, T.Y. and Mann, S. Synthetic cellularity based on non-lipid micro-compartments and protocell models. Curr Opin Chem Biol. 1-11 (2014)

[7] Booth, J.M., Restrepo Schild, V., Box, S.J. and Bayley, H., Light-patterning of synthetic tissues with single droplet resolution. Sci. Rep. 7, 9315 (2017)

[8] Hanczyc, M.M., Droplets: unconventional protocell model with life-like dynamics and room to grow. Life 4(4) 1038–1049 (2014).

[9] Cejkova, J., Novak, M., Štěpánek, F. and Hanczyc, M.M., Dynamics of chemotactic droplets in salt concentration gradients. Langmuir 30 11937-11944 (2014).

[10] Eisenbach, M., Chemotaxis. 499 Imperial College Press (2004).

[11] Pfeffer, W., Locomotorische richtungsbewegungen Durch chemische reize. Unters Bot. Inst.Tübingen 1,363 (1884)

[12] Bennett, R.R., Golestanian, R., A steering mechanism for phototaxis in chlamydomonas. Journal of The Royal Society Interface 12 (2015)

[13] Polyakova, T., Zablotskii, V., Magnetization processes in magnetotactic bacteria systems. Journal of Magnetism and Magnetic Materials 293 365-370 (2005)

[14] Mori, I., Ohshima, Y., Neural regulation of thermotaxis in Caenorhabditis elegans. Nature 376 344-348 (1995).

[15] Adler, J., Shi, W., Galvanotaxis in a bacteria. Cold Spring Harbor Symposia on Quantitative Biology 53 23-25 (1988)

[16] Carter, S.B., Haptotaxis and the mechanism of cell motility. Nature 213 256-260 (1967)

[17] Roberts, A.M., Mechanisms of gravitaxis in chlamydomonas. The Biological Bulletin 210 78-80 (2006)

[18] Meyers, L.A., Bull, J.J., Fighting change with change: adaptive variation in an uncertain world. Trends in Ecology & Evolution 17 551-557 (2002)

[19] Collin, M., Schuch, R., Bacterial sensing and signaling. Karger (2009)

[20] Jeon, K.W., International review of cytology: a survey of cell biology. Elsevier Science (2007)

[21] Ševčíková, H., Čejková, J. Krausová, L., Přibyl, M., Štěpánek, F.and Marek, M., A new traveling wave phenomenon of *Dictyostelium* in the presence of cAMP. Physica D: Nonlinear Phenomena 239 879-888 (2010)

[22] Song, L., Nadkarnia, S.M., Boedeker, H.U., Beta, C., Bae, A., Francka, C., Rappele, W.J., Loomisf, W.F., Bodenschatz, E., *Dictyostelium discoideum* chemotaxis: Threshold for directed motion. European Journal of Cell Biology 85 981-989 (2006)

[23] Entschladen, F. and Zänker, K.S., Cell migration: signalling and mechanisms. Karger (2009)

[24] Martin, P., Wound healing-aiming for perfect skin regeneration. Science 276 75-81 (1997)

[25] Behar, TN., Li, YX ., Tran, HT., Ma, W., Dunlap, V., Scott, C. and Barker, J.L., GABA stimulates chemotaxis and chemokinesis of embryonic cortical neurons via calcium-dependent mechanisms. The Journal of Neuroscience 16(5) 1808-1818 (1996)

[26] Howse, J. R. et al. Self-motile colloidal particles: From directed propulsion to random walk. Physical Review Letters 99 (2007)

[27] Roussos, E.T., Condeelis, J.S. and Patsialou, A., Chemotaxis in cancer. Nature Reviews Cancer 11 573-587 (2011)

[28] Solis, K. J. & Martin, J.,E. Complex magnetic fields breathe life into fluids. Soft Matter 45 9136-9142 (2014)

[29] Nistor, V., Cannell, J., Gregorya, J. & Yeghiazarian, L. Stimuli-responsive cylindrical hydrogels mimic intestinal peristalsis to propel a solid object. Soft Matter 15 3582-3588 (2016)

[30] Lagerwall, J. P. F. & Scalia, G. A new era for liquid crystal research: Applications of liquid crystals in soft matter nano-, bio- and microtechnology. Curr. Appl. Phys. 12(6) 1387–1412 (2012)

[31] Menzel, A. M. Tuned, driven, and active soft matter. Phys. Rep. 554 1–45 (2015)

[32] Toyota, T., Maru, N., Hanczyc, M.M., Ikegami, T., and Sugawara, T. Self-Propelled Oil Droplets Consuming “Fuel” Surfactant. J. Am. Chem. Soc. 131(14) 5012-2013 (2009)

[33] Hanczyc, M. M., Toyota, T., Ikegami, T., Packard, N. & Sugawara, T. Fatty acid chemistry at the oil-water interface: self-propelled oil droplets. J. Am. Chem. Soc. 129(30) 9386–9391 (2007)

[34] Lagzi, I., Soh, S., Wesson, P., Browne, K.P. & Grzybowski, B.A., Maze solving by chemotactic droplets. J. Am. Chem. Soc. 132(4) 1198-1199 (2010)

[35] Cejkova, J. *et al.*, Chemotaxis and chemokinesis of living and non-living objects. Springer, Advances in Unconventional Computing 256-260 (2016)

[36] Hanczyc, M.M. & Ikegami, T., Chemical basis for minimal cognition. Artif. Life 16(3) 233-243 (2010)

[37] Hanczyc, M.M., Metabolism and motility in prebiotic structures. Phil. Trans. R. Soc. B 366, 2885–2893 (2011)

[38] Holler, S., Porcelli, C., Ieropoulos, I.A. and Hanczyc, M.M., Transport of Live Cells Under Sterile Conditions Using a Chemotactic Droplet. Sci Rep 8:8408 (2018)

[39] Jin, C., Krüger, C, and Maass C.C., Chemotaxis and autochemotaxis of self-propelling droplet swimmers. PNAS (2017)

[40] Sakutal, H., Magome, N., Mori, Y. and Yoshikawa, K. Negative/positive chemotaxis of a droplet: Dynamic response to a stimulant gas. Appl. Phys. Lett. 108 (2016)

[41] Bormashenko, E., Liquid marbles: properties and applications. Curr. Opin. Colloid Interface Sci. 16(4) 266-271 (2011)

[42] Borges, J. *et al.* Biomaterials: nanoengineering hybrid supramolecular multilayered biomaterials using polysaccharides and self-assembling peptide amphiphiles. Adv. Funct. Mat. 27(17) (2017)

[43] Remminghorst, U., Bacterial alginates: from biosynthesis to applications. Biotechnol. Lett. 28, 1701-1712 (2006)

[44] Lee, K. Y. & Mooney, D. J. Alginate: properties and biomedical applications. Prog. Polym. Sci. 37(1) 106–126 (2012)

[45] Sambanis, A. Encapsulated islets in diabetes treatment. Diabetes Technol. Ther. 5(4) 665-668 (2003)

[46] Paltiel, H. J., Diamond, D. A., Zurakowski, D., Drubach, L. A. & Atala. A. Endoscopic treatment of vesicoureteral reflux with autologous chondrocytes: postoperative sonographic features. Radiology 232(2) 390-397 (2004)

[47] Murua, A., Orive, G., Hernandez, R.M. and Pedraz, J.L. Xenogeneic transplantation of erythropoietin-secreting cells immobilized in microcapsules using transient immunosuppression. J. Control. Release 137, 174 – 178 (2009)

[48] Bhujbal, S.V., de Vos, P. and Niclou, S.P. Drug and cell encapsulation: Alternative delivery options for the treatment of malignant brain tumors. Adv. Drug Del. Rev. 67-68 142-153 (2014)

[49] Gryshkov, O., Pogozhykh, D., Hofmann, N. and Glasmacher, B., Cell Encapsulation into Alginate Micro-Capsules Provides Living Cells with a Mild Environment During Cryopreservation. Cryobiology 66(3) (2013)

[50] Honghyun, P., Hyun Ji, L., Hyoseok, A. & Kuen Yong, L., Alginate hydrogels modified with low molecular weight hyaluronate for cartilage regeneration. Carbohydr. Polymers 162(1) 100–107 (2017)

[51] Mano, J.F., Stimuli-responsive polymeric systems for biomedical applications. Adv. Eng. Mat. 10(6) (2008)

[52] Pinto, S. *et al.*, Poly(dimethyl siloxane) surface modification by low pressure plasma to improve its characteristics towards biomedical applications. Colloids Surf. 81(1) 20-26 (2010)

[53] Zou, L. *et al.*, Surface hydrophilic modification of RO membranes by plasma polymerization for low organic fouling. J. Membr. Sci. 369(1) 420-428 (2011)

[54] Yi, C., Li, C.W., Ji, S. & Yang, M., Microfluidics technology for manipulation and analysis of biological cells. Anal. Chim. Acta 560(1-2) 1-23 (2006)

[55] Hanczyc, M. M., Parrilla, J. M., Nicholson, A., Yanev, K. & Stoy, K., Creating and maintaining chemical artificial life by robotic symbiosis. Artif. Life 21(1) 47-54 (2015)

[56] Biral, F., Bertolazzi, E., Bosetti, P., De Marchi, A. & Hanczyc, M.M., Optimal control of a laser source to generate a minimum time trajectory of a droplet in a liquid layer. In Future Technologies Conference (FTC) 1208-1216 (2016)

[57] Ieropoulos, J. A., Greenman, J., Melhuish, C. & Hart, J., Energy accumulation and improved performance in microbial fuel cells. J. Power Sources 154(2) 253-256 (2005)

[58] Zhao, F. *et al.*, Activated carbon cloth as anode for sulfate removal in a microbial fuel cell. Environ. Sci. Technol.42(13) 4971-4976 (2008)

[59] Shapiro, D.L., Nardone, L.L., Rooney, S.A., Motoyama E.K., and Munoz, J.L., Phospholipid biosynthesis and secretion by a cell line (A549) which resembles type II alveolar epithelial cells. Biochimica et Biophysica Acta (BBA) -Lipids Metabolism 530 (2) 197-207 1978

[60] W. Bernhard, Lung surfactant: Function and composition in the context of development and respiratory physiology. Ann Anat. 208 146-150 (2016)

[61] Parrilla Gutierrez, J.M., Hinkley, T., Taylor, J.W., Yanev, K. and Cronin L; Evolution of oil droplets in a chemorobotic platform. Nat Comun (2014)

[62] Kreja, L. and Seidel H-J, On the cytotoxicity of some microbial volatile organic compounds as studied in the human lung cell line A549. Chemosphere 49(1) 105-110 (2002)

[63] M.C. Potter, Electrical effects accompanying the decomposition of organic compounds. Proc. R. Soc. 84 260-276 (1911).

[64] Logan, B.E. et al. Microbial Fuel Cells: Methodology and Technology. 40(17) Env. Sci. Tec. 5181-5192 (2016).

[65] I.A. Ieropoulos, C. Melhuish, J. Greenman, Artificial metabolism: towards true energetic autonomy in artificial life. European conference in artificial life, Lect. Notes Artif. Intell. 2801 (2003) 792e799.

[66] I.A. Ieropoulos, J. Greenman, C. Melhuish, Int. J. Hydrogen Energy 38 492e496 Miniature microbial fuel cells and stacks for urine utilisation. (2013)

[67] Parrilla Gutierrez J.M., Hinkley, T., Taylor, J.W., Yanev, K. and Cronin, L., Evolution of oil droplets in a chemorobotic platform. Nat. Com. 5:5571 (2014)

[68] `https://blogit.itu.dk/evoblissproject/`

[69] Kikuchi, A., Kawabuchi, M., Sugihara, M., Sakuraia, Y. and Okano. T., Pulsed dextran release from calcium-alginate gel beads. Journal of Controlled Release. 47(1) 21-29 (1997)

[70] Kikuchi, A., and Okano, T., Pulsatile drug release control using hydrogels. Advanced Drug Delivery Reviews 45(1) 53-77 (2002)

[71] Nikoo, A.M., Kadkhodaee, R., Ghorani, B., Razzaq, H. and Tucker, N., Electrospray-assisted encapsulation of caffeine in alginate microhydrogels. International Journal of Biological Macromolecules 116, 208-216 (2018).

[72] Ogbonna, J.C., Matsumura, M., Yamagata, T., Sakuma, H. and Kataoka, H., Production of micro-gel beads by a rotating disk atomizer. Journal of Fermentation and Bioengineering 68(1) 40-49 (1989)

[73] Caldorera-Moore, M. and Peppas, N.A., Advanced Drug Delivery Reviews. 61(15) 1391-1401 (2009)